brain sciences

MDPI

Review

Multimodal Imaging and Molecular Biomarkers of Co-Pathology Across the Parkinson's Disease–Dementia with Lewy Bodies Continuum

Davide Mascioli [1], Matteo Conti [1], Tommaso Schirinzi [1] and Alessandro Stefani [1,2,*]

[1] Neurology Unit, Department of Systems Medicine, Tor Vergata University of Rome, 00133 Rome, Italy; matteoconti92@gmail.com (M.C.); t.schirinzi@yahoo.com (T.S.)
[2] Unità Operativa Semplice Dipartimentale Parkinson, Tor Vergata University Hospital, 00133 Rome, Italy
* Correspondence: stefani@uniroma2.it; Tel.: +39-06-72596010

Abstract

Parkinson's disease (PD) and dementia with Lewy bodies (DLB) are increasingly viewed as regions of a single α-synuclein continuum rather than separate entities. Neuropathology shows that Lewy pathology rarely occurs alone: Alzheimer-type amyloid-β and tau, transactive response DNA-binding protein 43 kDa (TDP-43) inclusions, and cerebrovascular lesions accompany it as the rule rather than the exception, and this co-pathology contributes to the clinical heterogeneity observed across the continuum without mapping onto its clinical divisions. The open problem is no longer whether co-pathology matters but how to measure it in living patients and integrate that information for individualized care. This review is organized by proteinopathy (α-synuclein as the primary lesion, then amyloid-β, tau, and TDP-43/vascular co-pathology) and, within each, follows the modalities that interrogate it: molecular imaging, fluid and tissue biomarkers, and their downstream structural, metabolic, functional, and electrophysiological correlates. No single technique captures the co-pathological landscape. Profiling an individual's proteinopathy burden in vivo requires a deliberate combination of methods, and precision management of the PD–DLB continuum depends on this multimodal integration.

Keywords: biomarkers; α-synuclein; co-pathology; seed amplification assay; amyloid-β; tau PET; TDP-43; cerebrovascular

1. Introduction

Parkinson's disease (PD) and dementia with Lewy bodies (DLB) are the two most common Lewy body (LB) diseases, and their operational separation, most often by the "one-year rule" distinguishing DLB from PD dementia (PDD), has always been pragmatic rather than biological [1,2]. Diagnostic criteria on both sides of the continuum, from the Movement Disorder Society criteria for PD and prodromal PD [3,4] to the fourth consensus report of the DLB Consortium [1], have mutated, and PD and DLB are increasingly conceptualized as one disease spectrum [5,6]. Cognitive impairment, the feature that most strongly marks a position on that continuum, is itself a major determinant of prognosis and care burden [7].

In this Lewy body disease spectrum (LBDS), the defining lesion is the accumulation of aggregated α-synuclein (α-syn) in LB, but it rarely occurs alone [8,9]. Autopsy series consistently show that the majority of people with PD/DLB carry additional proteinopathies, and it is increasingly recognized that co-pathology is the rule in both idiopathic and monogenic

Check for updates

Academic Editor: Brenda Hanna-Pladdy

Received: 17 September 2026
Revised: 26 October 2026
Accepted: 28 October 2026
Published: 2 November 2026

Copyright: © 2026 by the authors. Licensee MDPI, Basel, Switzerland. This article is an open access article distributed under the terms and conditions of the Creative Commons Attribution (CC BY) license.

LB diseases, with amyloid-β (Aβ) plaques, protein tau tangles, TDP-43, and cerebrovascular disease each linked to specific clinical features and outcomes [9]. Alzheimer's disease (AD) co-pathology in particular shifts the phenotype toward a faster cognitive decline course and shortens survival [10]. Thus, co-pathology represents an additional source of biological and clinical heterogeneity across the PD–DLB continuum.

The move toward biological definitions of LBDS, the neuronal α-syn disease integrated staging system (NSD-ISS) and the Synucleinopathy–Neurodegeneration–Genetics (SynNeurGe) framework [11–13], places α-syn and neurodegeneration on explicit, separable axes and conceptualizes PD and DLB as expressions of a single biological entity. These frameworks therefore allow the primary synucleinopathy to be considered alongside the co-pathologies that influence disease expression.

This narrative review examines how these proteinopathies can be detected and quantified in vivo across the PD–DLB continuum and how the available measures can be integrated. We organize the evidence by protein (α-syn first, then Aβ, tau, and TDP-43/vascular co-pathology) and, within each, walk through molecular imaging, fluid and tissue biomarkers, and downstream imaging and electrophysiological correlates. We identified relevant literature through searches of PubMed and Scopus for articles published between 2004 and 2026. Search strings combined three broad blocks of terms: the clinical spectrum ("Parkinson's disease", "Parkinson's disease dementia", "dementia with Lewy bodies", "Lewy body disease", "synucleinopathy", "prodromal Parkinson's disease", "REM sleep behavior disorder", "mild cognitive impairment"); the target pathology ("α-synuclein", "amyloid", "tau", "transactive response DNA-binding protein 43 kDa (TDP-43)", "TDP-43", "limbic-predominant age-related TDP-43 encephalopathy", "cerebrovascular", "small vessel disease", "cerebral amyloid angiopathy", "co-pathology", "mixed pathology", "neurodegeneration"); the measurement modality ("positron emission tomography" (PET), "single-photon emission computed tomography" (SPECT), "magnetic resonance imaging" (MRI), "diffusion", "electroencephalography" (EEG), "cerebrospinal fluid" (CSF), "plasma", "serum", "seed amplification assay", "skin biopsy", "biomarker", "neuropathology"). Priority was given to peer-reviewed original studies, systematic reviews and meta-analyses published in English, and, among these, to neuropathologically validated cohorts, large or multicenter studies, and longitudinal designs. Studies in other neurodegenerative diseases and selected experimental work were also considered where they informed the interpretation or the technical limits of a biomarker in this population. As this is a narrative review, study selection reflected the authors' judgment of relevance; therefore, no systematic search protocol was applied.

2. The Hallmark: α-Synuclein Detection In Vivo

α-syn is a small presynaptic protein encoded by SNCA, physiologically involved in synaptic vesicle trafficking and neurotransmitter release [14]. Its misfolding and aggregation into LB and Lewy neurites define PD and DLB neuropathologically [15], with a regional distribution that varies between the two clinical entities and, within each, over the disease course [16].

2.1. Molecular Imaging of α-Syn

No PET tracer for aggregated α-syn has yet been validated for clinical use. First-generation compounds bind α-syn selectively over Aβ and tau fibrils in model systems, and structural work has clarified their binding mode [17], prompting the view that such tracers could transform diagnosis and therapeutic monitoring [18]. The only ligand with substantial clinical characterization is [^{18}F]ACI-12589, which has shown promising results in the individuation of patients affected by another synucleinopathy, multiple system atrophy

(MSA) [19]. Retention in PD and DLB, by contrast, was limited, and whether this reflects the lower lesion density of LB or the distinct conformation of the α-syn fold remains unresolved; interestingly, the elevated signal seen in two SNCA-duplication carriers, in whom α-syn burden is high, is at least compatible with a density threshold [19,20]. The main problem for other tracers is selectivity. A tracer meant to quantify α-syn burden in the presence of Aβ and tau aggregates must not bind them, yet all three share a cross-β architecture [21]. [^{18}F]ACI-12589 retention has been reported in disease-affected regions of AD patients, and independent autoradiographic work has since documented that [^{3}H]ACI-12589 binds to amyloid-β plaques [22]. Of the other compounds that have produced an MSA signal ([^{18}F]SPAL-T-06, [^{11}C]MODAG-005, [^{18}F]C05-05), each shows in vitro affinity for amyloid-β and/or tau, and [^{11}C]MK-7337 and [^{11}C]SY08 carry a substantial off-target cortical or vascular signal [20]. Higher-affinity successors are in development, and dedicated reviews catalogue the tracer-development effort and its hurdles [23–25]. At present, α-syn PET is not ready to be part of current practice.

2.2. α-Syn Quantification and Seed-Amplification Assays in Fluids and Tissue

Direct quantification of total, phosphorylated (Ser129), or oligomeric α-syn in CSF and blood has failed to separate LBDS from controls or from other Parkinsonian syndromes.

Meta-analyses converge on a modest reduction in CSF total α-syn in PD relative to controls, with no difference across PD, DLB, and MSA, and overlapping distributions that preclude individual classification. Moreover, CSF total α-syn does not differ significantly from PD in corticobasal syndrome and vascular parkinsonism, where α-syn misfolding is not the driver [26–28]. pS129 α-syn and oligomeric α-syn, despite being the dominant species within LB, have shown no better results [29]. Blood-based studies on α-syn have yielded inconsistent findings, with total α-syn in plasma/serum having been reported as increased, decreased, or unchanged in PD compared with controls [26]. Moreover, roughly 99% of total α-syn in the blood is carried by erythrocytes, so hemolysis is a major confounding factor in this kind of assay [30]. Other blood cell populations have also been examined: an accumulation of oligomeric α-syn has been reported in peripheral blood mononuclear cells in PD, with total α-syn unchanged [31].

In contrast to its quantification in biofluids, the immunohistochemical detection of pS129 α-syn in peripheral tissue has shown high diagnostic yield. In skin biopsies, pS129 α-syn deposits within cutaneous nerve fibers are visualized by immunofluorescence, and in a blinded 30-site study, they were detected in 92.7% of patients with PD and 96.0% of patients with DLB, compared with 3.3% of controls [32]. In a subgroup analysis of the same cohort, cutaneous pS129 α-syn was also found in almost a third of control participants with cognitive impairment [33], indicating that peripheral α-syn deposition can be present in cognitively impaired individuals who do not meet clinical criteria for DLB. As currently applied, the test reports the presence of deposits rather than their central burden, and its relationship with co-pathology is being addressed in an ongoing prospective study that pairs skin biopsy with plasma p-tau217 in mild cognitive impairment [34].

A major recent advance has been the direct detection of misfolded α-syn using seed-amplification assays (SAA), implemented as real-time quaking-induced conversion or protein-misfolding cyclic amplification [35,36]. Diagnostic performance is high, even with differences depending on the biological matrix, across CSF, skin, blood, olfactory mucosa, and extracellular vesicle preparations [37,38]. Assay development is now focused on improving analytical performance and practicality, including the choice of biological source and detection strategy [39,40]. This technique has several limitations. First, the assay is dichotomous by design: its kinetic parameters are not calibrated measures of seed burden, and positivity thresholds vary across laboratories [38]. Approaches to move beyond this

dichotomy are under development: kinetic measures such as time-to-threshold carry diagnostic and prognostic information, such as predicting cognitive decline in PD [41], and endpoint-dilution and immunoassay-based formats now estimate seed concentration [42], with seeding doses that correlate with LB pathology load at autopsy [43]. The second one is that, despite being the hallmark of LBDS, misfolded α-syn can be detected by SAA in other neurodegenerative diseases, in particular AD, which is known for carrying synucleinopathy co-pathology in almost 50% of cases [44]. Despite this, SAA is the only technique that can qualitatively establish the presence of misfolded α-syn. Importantly, most of the current SAAs confirm α-syn pathology across the spectrum but do not, on their own, separate PD from DLB. Regarding this caveat, using conformation-selective antibodies, a recent study found plasma levels of two strain-like α-syn species to be higher in PD than in DLB in two independent cohorts [45].

Cell-based assays provide a complementary, though still experimental, readout of α-syn strain properties. In Förster resonance energy transfer (FRET) biosensor cells expressing fluorescently tagged α-syn, seeded aggregation generates a FRET signal that can be quantified at the single-cell level. Applied to SAA-amplified seeds from patient skin, this approach showed that PD-derived strains induce a greater intracellular burden and a distinct pS129-positive inclusion morphology compared with DLB-derived strains [46]. In autopsy-confirmed PD, biosensor seeding activity correlated with insoluble pS129 α-syn levels and varied widely between individuals [47].

3. Aβ Co-Pathology In Vivo

Aβ plaques, together with tau neurofibrillary tangles, constitute the pathological signature of AD [48]. In LBDS, Aβ is the most frequently measured co-pathology and, with tau phosphorylated at threonine 181 (p-tau181), the best characterized in living patients [49,50]. Its presence is a prognostic modifier; indeed, co-existing AD pathology is associated with accelerated cognitive and functional decline, higher mortality, and poorer treatment response [10]. Unlike the fluid α-syn markers discussed above, Aβ can be quantified in vivo with concordant, well-validated tools, which makes it the prototypical measurable co-pathology.

3.1. Molecular Imaging of Aβ

Amyloid PET provides a direct, topographical readout of cortical fibrillar Aβ [51,52]. Antemortem retention corresponds to what is found at autopsy: in LBDS, global cortical [^{11}C]Pittsburgh compound B ([^{11}C]PiB) retention corresponds to Thal phase and to neuritic and total plaque burden [53,54], and regional binding of the ^{18}F-labeled amyloid PET tracers used in clinical practice matches regional Aβ immunohistochemistry in a small autopsy series [55]. This relationship also extends beyond amyloid, since ([^{11}C]PiB) retention also scales with Braak neurofibrillary tangle stage and with LB scores [54], so the measure is not independent of the primary pathology when the two accumulate together.

This positivity is unevenly distributed across the continuum. It is negligible in non-demented PD [56] and, at the prodromal stage of isolated rapid eye movement sleep behavior disorder (iRBD), indistinguishable from that of cognitively unimpaired controls. Across [^{11}C]PiB studies, roughly 5% of PD with mild cognitive impairment (PD-MCI) scans are positive, rising to around a third in PDD and two-thirds in DLB [57], with cortical burden increasing along the DLB continuum [58,59]. On the DLB side, the rise begins earlier: about a third of patients with mild cognitive impairment with Lewy bodies (MCI-LB) are already amyloid positive, against the 5% recorded at the corresponding stage on the PD side [60]. Across non-AD dementias, DLB included, the likelihood of a positive scan rises with age and apolipoprotein E (APOE) ε4 carriership [59,61]. Prevalence estimates vary

with tracer and threshold. A PET/MRI series using [^{18}F]flutemetamol found significant deposition in half of PDD and half of DLB patients, with an overall prevalence of about a third across Lewy body disease [62], concordant with meta-analytic figures for PDD but appreciably lower for DLB [57].

The method used to define PET positivity may be as important as the tracer itself. In fact, in DLB, visual rating of amyloid positivity was associated with subsequent clinical decline, whereas the continuous cortical uptake ratio from the same scans was not [63]. Where amyloid is detected, its regional distribution in LBDS is cortical and subcortical rather than restricted to the regions typical of AD. In PD-MCI imaged with [^{18}F]flutemetamol, deposition involved the middle frontal cortex, precuneus, and paracentral regions and, bilaterally, the putamen, with no accompanying difference in grey-matter volume between amyloid-positive and amyloid-negative patients [64]. In another study, [^{18}F]florbetaben uptake in PD clustered differently from controls, and higher occipital and parietal uptake was associated with lower Montreal Cognitive Assessment (MoCA) scores [65]. Structural differences were less evident, as the presence of amyloid was not accompanied by an AD-type atrophy pattern or by a difference in vascular load on visual rating [62].

3.2. Fluid Amyloid Biomarkers

Alongside the amyloid PET, a low CSF level of Aβ42, or, more robustly, a low Aβ42/40 ratio, is the best-validated fluid index of cortical amyloid [66], and it predicts cognitive decline at every point along the LBDS. In newly diagnosed, untreated PD, baseline Aβ42 was lower in patients who became cognitively impaired within two years [67]; in treated PD, those below the Aβ42 threshold declined substantially faster [68]; in DLB, pathological Aβ42 predicted a steeper fall in Mini-Mental State Examination (MMSE) [69]. Prospective data up to ten years in a population-based cohort showed high CSF neurofilament light chain together with low Aβ42 predicted conversion to PDD [70]. In these cohorts, the prognostic signal is carried mainly by Aβ42. A systematic review of 31 studies confirmed the direction of effect: among those judged at low risk of bias, AD co-pathology was associated with accelerated cognitive and functional decline, greater mortality, and poorer treatment response, and no study reported better outcomes in its presence [10]. Combining Aβ42 with synaptic markers sharpens this further: paired with neurogranin, it correlates with global cognition in PD and separates cognitively impaired from unimpaired patients more accurately than neurogranin alone [71]. Adding CSF SAA to CSF Aβ42 status splits PD into four groups with distinct trajectories: dual-positive patients decline fastest, and each step in combined status nearly triples the hazard of dementia [72].

Two features of the measure itself qualify these results. Thresholds in current use were derived in AD patient cohorts and may underestimate amyloid pathology in the LBDS, which has prompted calls for disease-specific cut-offs [73]. In addition, Aβ42 may behave differently when a second proteinopathy is present; indeed, in a large memory-clinic series, CSF Aβ42 was higher in AD with LB comorbidity than in pure AD, and most patients carrying both diagnoses showed elevated tau and p-tau alongside a normal Aβ42 [74].

Blood-based markers now extend this to scalable, screening-compatible stratification, though in blood, it is phosphorylated tau (p-tau181, p-tau217) rather than Aβ42 itself that most reliably reflects brain amyloid status [75,76]. In PD, serum/plasma Aβ42 does not differ from that of healthy controls [77] but is lower in patients with amnestic cognitive impairment [78]. In DLB, plasma Aβ42/40 ratio and p-tau181/231 discriminate amyloid-positive from amyloid-negative patients without tracking cognitive decline over time [79]. Concentration of p-tau181 is higher in DLB with intermediate or high AD neuropathologic change yet unrelated to LB Braak stage or to tau-PET uptake [80]. The signal is not uniform across cohorts, since one series found plasma glial fibrillary acidic protein (GFAP), but not

p-tau181, elevated in LBDS with concomitant AD change [81]. At the prodromal stage, plasma p-tau181 together with Aβ42 markers predicts conversion to dementia in iRBD cohorts [82], and combined amyloid-tau biomarker profiles further help define the clinical phenotype of DLB [83].

4. Tau Co-Pathology In Vivo

Tau is a microtubule-associated protein that aggregates into neurofibrillary tangles when hyperphosphorylated [84]. Alongside Aβ plaques, it constitutes AD co-pathologies, and among PD co-pathologies, it is the one most strongly associated with cognitive decline [9].

4.1. Molecular Imaging of Tau

In LBDS, cortical tau on PET is generally low and appears largely conditional on amyloid presence. Across the continuum, it rises from non-demented PD to PDD and DLB, scaling with amyloid burden and cognitive impairment [85,86]. This relationship appears to be asymmetric: when patients are scanned for both proteins, no cortical region shows elevated tau binding in any amyloid-negative group, whether in PD with normal cognition, PDD, or DLB, whereas within DLB, occipital tau tracks local amyloid [85]. The second-generation tracer [^{18}F]PI-2620 shows the same dependence in different regions, since its uptake correlates with amyloid PET in the temporal cortex and precuneus, and inferior temporal signal is higher in amyloid-positive than amyloid-negative patients with LBDS [87]. In addition, affinity is isoform dependent, higher for the mixed three- and four-repeat deposits of AD than for three- or four-repeat pathology alone [88], leaving non-AD tauopathy largely unmeasured.

Amyloid can be present in the absence of neocortical tau, whereas neocortical tau is rarely detected without amyloid; the two contribute to neurodegeneration in probable DLB in a region-specific rather than interchangeable manner [89]. The apparent burden of tau pathology also depends on the tracer, and findings have not been fully consistent across studies. With [^{18}F]flortaucipir, deposition in DLB is minimal [90,91], whereas with [^{18}F]PI-2620, cortical uptake in LBDS is low overall and far below that of AD, yet the small elevations present correspond to executive function and attention rather than to memory [87]. With [^{18}F]florzolotau, tau in DLB appears widespread and topographically heterogeneous, with just over half of patients showing AD-like spatial patterns and a smaller group showing a pattern distinct from AD [92]. When detected, tau burden is associated with both clinical progression and structural degeneration. In fact, it accumulates longitudinally in step with cortical atrophy and cognitive decline [93], and baseline burden accelerates atrophy of AD-vulnerable hippocampal parts in a way that amyloid alone does not [94]. In addition, tau-related cortical microstructural change follows the same co-pathological pattern [95]. Two limitations qualify these findings. First, tau binding correlates only weakly with clinical status in DLB; in one series, regional hypoperfusion derived from the same dynamic scan tracked cognition more closely than tau binding itself [96]. Second, the [^{18}F]flortaucipir visual read approved for AD classifies only a minority of amyloid-positive DLB patients as tau-positive [97], reflecting the low tau burden typical of this population.

4.2. Fluid Tau Markers

CSF and plasma p-tau species complement imaging and, unlike PET, are suitable for standard practice. In CSF, total tau and phosphorylated tau are unchanged or even reduced in PD relative to controls and remain so as Aβ42 falls in PD with cognitive impairment or PDD, where almost one-half of patients nonetheless display the AD CSF signature [98,99]. In initially untreated PD, baseline p-tau and p-tau/Aβ42 forecast subsequent memory and

executive decline once follow-up begins [100], and a high CSF p-tau/total-tau (t-tau) ratio at onset predicts the later development of motor complications [101]. Prognostic accuracy improves further when a marker of neurodegeneration is added. For example, in early PD, CSF Aβ42 and p-tau181 together with serum neurofilament light identify the patients who decline fastest [102]. In DLB, the same CSF profile, including elevated p-tau, identifies co-existing AD pathology and relates to cognitive and neurodegenerative severity [83]. To add a layer of complexity, antemortem CSF t-tau/Aβ42 and Aβ42 predict the burden of cortical α-syn at autopsy, not only of tau and amyloid [103].

Under current criteria for AD, soluble p-tau181 and p-tau217 are early-changing markers of AD neuropathologic change, whereas tau PET indexes neocortical tangle burden [104]. In blood, p-tau detects amyloid more accurately than the amyloid peptides themselves [75]. Plasma p-tau181 and p-tau217 identify amyloid co-pathology within DLB, and across large multicenter cohorts, plasma p-tau181 is the strongest single marker separating amyloid-positive from amyloid-negative DLB [105,106]. In PD, plasma p-tau217 identifies AD co-pathology with comparable accuracy [107], and across the continuum, its concentration rises with the relative weight of the two proteinopathies rather than registering the presence of either [108].

5. TDP-43 and Vascular Co-Pathology

5.1. TDP-43 Co-Pathology

TDP-43 is a nuclear DNA- and RNA-binding protein that mislocalizes to the cytoplasm and aggregates as hyperphosphorylated inclusions in amyotrophic lateral sclerosis, frontotemporal lobar degeneration, and, in its age-related limbic form, limbic-predominant age-related TDP-43 encephalopathy (LATE) [109]. TDP-43 aggregates occur in a substantial minority of LBDS, close to a third of DLB cases and over half of those with mixed AD and Lewy pathology, rising with neocortical LB burden and with concomitant AD-related change [110,111]. Its presence also hinders clinical detection: in cases of autopsy-confirmed transitional or diffuse Lewy body disease, hippocampal TDP-43 is linked to the likelihood of not receiving a probable DLB diagnosis during life, regardless of advanced age at death and a significant Braak neurofibrillary tangle stage [112]. In PDD autopsy reviews, TDP-43 pathology did not generally explain dementia as strongly as cortical α-syn, amyloid, and tau [113]. The co-pathology is not as the manifestation observed in AD. In DLB, LATE presents a distinct hippocampal distribution compared to AD, with neuronal cytoplasmic inclusions more commonly found in CA3 and numerous fine neurites of C-terminally truncated TDP-43 extending from CA2 to the subiculum, some of which colocalize with phosphorylated α-syn, and its occurrence and severity correlate with cognitive impairment [114]. No validated in vivo TDP-43 tracer yet exists. The first candidate PET ligands are only now being characterized at the preclinical stage [115,116]. Fluid markers are at a comparable stage. An ultrasensitive CSF assay for tau acetylated at lysine 174 separates FTLD-TDP from FTLD-tau, but the same marker is raised in every dementia group examined, DLB included, so its elevation does not index TDP-43 specifically, and it has not been evaluated as a marker of TDP-43 co-pathology within Lewy body disease [117]. TDP-43 can therefore at best be inferred indirectly, from an amnestic syndrome with disproportionate hippocampal atrophy in the absence of sufficient amyloid, as formalized in proposed but still unvalidated LATE clinical criteria [118], or from cortical microstructural diffusion measures, which are further reduced where Lewy or TDP-43 co-pathology accompanies AD change [119].

5.2. Cerebrovascular Co-Pathology

Cerebrovascular disease is common across the LBDS continuum and, unlike TDP-43, is directly visible on structural MRI and quantifiable with established small-vessel-disease scores [120]. Its clinical consequences are both direct and synergistic. A greater small-vessel burden is associated with worse motor impairment in PD [121], its progression tracks cortical thinning and parallel cognitive decline [122], and macroinfarcts and atherosclerosis interact with LB pathology to worsen parkinsonism beyond what either produces alone [123]. Part of this vascular-hemorrhagic burden, however, is not hypertensive but amyloid in origin. Cerebral amyloid angiopathy is present in the large majority of DLB but only a minority of non-demented PD and carries a worse prognosis tied to both tau stage and angiopathy severity [124]. Lobar cerebral microbleeds occur in DLB at a prevalence resembling AD, though with wide variation across series [125], and where the two are compared directly, white-matter hyperintensities in DLB correspond to AD-related change rather than to atherosclerotic vasculopathy [126]. Impaired perivascular clearance has been proposed as a further contributor. Thalamic free water is elevated in PD and correlates inversely with a diffusion index of glymphatic function [127], and free-water change in cognition-related thalamic nuclei accompanies cognitive decline [128]; whether either relates to α-syn accumulation remains untested.

6. Downstream Markers: Co-Pathology from Imaging and Electrophysiology

The preceding sections focused on methods for detecting protein pathology, whereas this section considers its downstream effects. Structural, functional, electrophysiological, and metabolic imaging; synaptic and neuroinflammatory PET; and fluid markers of neuroaxonal injury index the net neurodegenerative and network burden of accumulated pathology. None is intrinsically specific to a single proteinopathy. A downstream signal serves as a marker of co-pathology only when connected to a molecular or fluid measure.

6.1. Signatures of the Primary Synucleinopathy

Dopaminergic imaging occupies a particular position among these markers. *N*-ω-fluoropropyl-2β-carbomethoxy-3β-(4-[^{123}I]iodophenyl)nortropane ([^{123}I]FP-CIT) SPECT measures presynaptic dopamine transporter density and therefore reflects nigrostriatal terminal loss, a core element of LBDS. Compared with autopsy findings, it distinguishes LBDS from AD with good accuracy, even if a normal scan does not exclude LBDS, since in around 10% of pathologically confirmed cases, normal scans were associated with mild nigral cell loss but moderate cortical α-synuclein pathology [129]. In another autopsy series, normal scans were more frequent in women, who also showed more AD co-pathology; in the same study, semiquantitative analysis improved detection [130]. Moreover, [^{123}I]FP-CIT abnormalities are not specific to LBDS and can also occur in PSP, corticobasal degeneration, MSA, and frontotemporal lobar degeneration [129]. Within PD, caudate uptake is more closely related to cognition and predicts subsequent executive and visuospatial decline in de novo patients [131]. This appears largely independent of amyloid status: β-amyloid PET and [^{123}I]FP-CIT identify largely non-overlapping biomarker profiles in MCI at risk for Lewy body dementia [60].

At the structural level, atrophy evolves along the continuum. It is minimal in non-demented PD and greater in the demented phenotypes, with hippocampal and parahippocampal loss greater toward the DLB end than in non-demented PD [132] and with cortical topography shifting between the two dementia poles, bilateral frontal atrophy with reduced frontal coherence toward PDD and predominantly parietal atrophy with reduced posterior connectivity toward DLB [133]. Subcortically, hippocampal atrophy accompanies the PD-to-PDD transition, while pallidal volume differs between the two dementia poles [134].

Imaging of the substantia nigra provides one of the closest structural correlates of the primary lesion. Neuromelanin-sensitive imaging depicts catecholaminergic cell loss [135], and loss of dorsolateral nigral hyperintensity, the swallow-tail sign, on susceptibility-weighted imaging is abnormal across the LBDS and separates DLB from other dementias with moderate accuracy in meta-analysis [136]. Measures of the basal forebrain and brainstem are abnormal already in the prodromal and predementia stages: nucleus basalis of Meynert grey-matter volume reduction in early PD and in iRBD is associated with cognitive and symptom burden and predicts conversion to dementia in PD and phenoconversion in iRBD [137]. Neuromelanin signal in the caudal locus coeruleus is reduced in MCI-LB and is associated with visuospatial impairment [138]. Quantitative susceptibility mapping refines the iron measure further: nigral susceptibility tracks LB pathology at autopsy [139], follows a prodromal-to-clinical gradient [140], and differs between the two dementia poles across multiple regions, scaling with overall disease severity [141].

At the network level, functional MRI maps the dysfunction underlying cognitive and neuropsychiatric symptoms [142]. Attention and fronto-parietal hypoconnectivity are reported across α-synucleinopathy [143], with systematic reviews converging on reduced network efficiency [142,144,145] and only subtle DLB–PDD differences consistent with a shared substrate [133,146], while cholinergic-hub connectivity of the nucleus basalis of Meynert is informative for the cognitive phenotype [147,148]. Findings vary across acquisition and analysis approaches [149–151], which tempers single-subject use.

Electrophysiology contributes an inexpensive, dynamic readout matched to the fluctuating core of DLB. Posterior slowing of the dominant rhythm into the pre-alpha band, interpreted as thalamocortical dysrhythmia, is present in roughly 90% of DLB cases across systematic reviews [152,153], emerges early in the dementia course [154,155], correlates with cognitive fluctuations [156], and is recognized among supportive diagnostic features, with frontal rhythmic delta activity as an accessible visual adjunct [157]. High-density and source-resolved approaches extend this to network-level signatures already abnormal at the MCI stage [158]. The pathophysiology of these fluctuations has been synthesized into an integrative arousal-network framework spanning EEG, fMRI and diffusion measures [159].

Metabolic imaging contributes a further primary-process signature. On [^{18}F]fluorode oxyglucose PET ([^{18}F]FDG-PET), the demented phenotypes show posterior, occipital and parieto-occipital hypometabolism, with relative preservation of the posterior cingulate against the surrounding precuneus and cuneus, the cingulate island sign [160], which is part of the supportive biomarkers for DLB [1].

6.2. Imaging Signatures of Co-Pathologies

AD co-pathology is associated with regionally specific patterns of structural change on MRI that can be validated against molecular PET. Validated against [^{11}C]PiB and [^{18}F]flortaucipir, the contributions of amyloid, tau and cerebrovascular disease to grey-matter loss in probable DLB are regionally specific and separable, even though most cortical atrophy remains attributable to α-syn-related pathology. Specifically, amyloid load maps preferentially to inferior-temporal volume loss [89], while cerebrovascular burden maps to medial and orbital frontal, insular and thalamic atrophy on a path separable from that of amyloid and tau [89,161], although, as set out in Section 5.2, that burden cannot itself be assigned to a single vascular origin. Within the medial temporal lobe, the resolution improves, and the two proteins separate. Atrophy involves the hippocampal output subfields characteristic of AD, subiculum and CA1, with relative sparing of the CA2/3 subfields associated with Lewy pathology; subiculum volume mediates the association between amyloid and cognition, and baseline tau, rather than amyloid, is associated with faster longitudinal atrophy of CA1 and subiculum [94]. Parcellation of the whole medial temporal lobe gives

a broader distribution: LBDS with AD co-pathology shows atrophy across all subregions except the posterior hippocampus, with the largest effect in trans-entorhinal BA35 and entorhinal cortex, where entorhinal volume correlates with autopsy tau load [162]. The amyloid contribution may register as dysfunction before atrophy can be detected, since amyloid-positive and amyloid-negative DLB are clinically and volumetrically indistinguishable, differing only in medial temporal hypoperfusion [163].

At the network level, the evidence is thinner, and few studies directly isolate amyloid. Resting-state fMRI in DLB shows reduced posterior connectivity, but its coupling to metabolism is weak in multimodal data, and the available comparison sets amyloid-positive posterior cortical atrophy against amyloid-negative DLB [164]. Stratifying by a genetic determinant of AD co-pathology can be used as a proxy instead. In de novo PD, APOE ε4 carriers show an EEG-based connectivity pattern distinguishable from that of non-carriers, alongside differences in CSF amyloid markers [165]. Post-mortem work identifies a candidate substrate: amyloid-β load in the insula is associated with axonal degeneration, which in turn corresponds to cognitive status across PD, PDD and DLB [166]. Current synthesis places the amyloid contribution to connectivity failure on top of synuclein-related change, with functional disruption preceding atrophy and emerging in interaction with tau and cholinergic loss rather than as a standalone amyloid signature [167].

Metabolic imaging provides complementary information on functional impairment. [^{18}F]FDG PET declines longitudinally along the continuum in a pattern that parallels clinical progression and has been referenced to post-mortem neuropathology [168]. The two processes appear to leave partially distinct spatial signatures. The occipital component belongs to the synucleinopathy: where individuals spanning the AD continuum are stratified by α-syn SAA, seeding positivity carries a posterior-dominant hypometabolic signature independent of CSF amyloid and tau, most clearly in the occipital cortex, and that regional hypometabolism mediates the association between SAA and clinical severity [169]. In contrast, posterior cingulate involvement appears to be more closely related to the AD-related process, since metabolic decline there, with erosion of the cingulate island sign, corresponds to tau accumulation rather than to amyloid load [170]. Consistent with an amyloid contribution that is real but indirect, glucose metabolism can fall in PD and PDD when the amyloid signal is only marginally raised [171], and across mixed dementias, [^{18}F]FDG PET is now read less as a categorical class label than as an index of the predominant underlying pathology [160].

The TDP-43 axis is approached differently, since no molecular anchor is available against which to validate a downstream signal. In autopsy-confirmed cases, TDP-43 positivity is associated with moderate-to-severe medial temporal atrophy on MRI and medial temporal hypometabolism on [^{18}F]FDG PET, with relative sparing of the parietal cortex [172]. Of particular interest is the disproportionate degree of atrophy in LATE, where limbic atrophy and hypometabolism exceed what the local burden of AD pathology would predict [173]. In addition, plasma TDP-43 tracks entorhinal and parahippocampal volume independently of AD biomarkers [174]. On downstream imaging, the effects of TDP-43 overlap substantially with those associated with amyloid and tau, and it can be inferred only as the fraction of medial temporal injury exceeding what amyloid and tau account for.

6.3. Fluid Markers of Neuroaxonal Injury

NfL is a structural protein of myelinated axons that is released into CSF and blood upon neuroaxonal damage, independently of the underlying cause [175]. It is therefore the fluid counterpart of the downstream imaging markers discussed above, reflecting the intensity of neurodegeneration but not the protein responsible for it. Within the LBDS, higher plasma NfL is associated with lower global cognition in PD and predicts subsequent

decline on the MMSE score [176], baseline levels predict the later emergence of psychotic symptoms [177], and, combined with low CSF Aβ42, high CSF NfL predicted conversion to PDD over up to ten years [70]. Its relationship with co-pathology is indirect. In a multicenter study, once amyloid-positive cases were excluded, GFAP and NfL were the only plasma markers that retained discriminative value for DLB [106], whereas in iRBD, serum NfL did not track cognitive scores and added little to p-tau217 in predicting phenoconversion to PDD or DLB [178]. Interpretation at the individual level must also account for age, body mass index, and renal function, which shift plasma concentrations independently of neurological disease [179]. NfL thus supplies the severity axis of a multimodal profile.

6.4. Synaptic and Neuroinflammatory PET

Synaptic vesicle glycoprotein 2A (SV2A), an integral membrane protein of presynaptic vesicles expressed across virtually all synapses, provides a PET target for synaptic density [180]. With [^{11}C]UCB-J, non-demented PD shows reduced binding largely confined to the substantia nigra, whereas PDD and DLB show widespread cortical reductions that correlate with executive performance [181]. The ^{18}F-labeled ligand [^{18}F]SynVesT-1, whose longer half-life broadens clinical applicability, has reproduced the [^{11}C]UCB-J findings in PD [182] and correlates closely with [^{11}C]UCB-J in head-to-head comparison in healthy volunteers [183]. Synaptic loss and hypometabolism are related in LBDS, but the reduction in [^{18}F]FDG PET uptake exceeds that of [^{11}C]UCB-J binding, so hypometabolism cannot be accounted for by synaptic loss alone [184].

Neuroinflammation in LBDS may be imaged through the 18 kDa translocator protein (TSPO), which is upregulated in activated microglia and reactive astrocytes [185]. [^{11}C]PK11195 binding is increased in cortical and subcortical regions in PDD and, to a lesser extent, in non-demented PD, in the presence of only a marginal amyloid signal [171]. In DLB, binding is highest at mild disease stages and declines as cognition worsens, with no regional correspondence with amyloid PET [186]. In early PD, regional binding is higher in patients at high risk of dementia and correlates with regional [^{18}F]flortaucipir signal, although tau binding itself is minimal [187], and nigral binding at baseline predicts cognitive decline over three years [188]. TSPO PET is nonetheless limited by a low specific signal and by the dependence of tracer affinity on a common polymorphism of the TSPO gene [185]. Like NfL, synaptic and neuroinflammatory PET quantifies processes shared across proteinopathies, and they become informative for co-pathology profiling only when anchored to molecular measures.

Table 1 summarizes, for each target pathology, the molecular, fluid, and downstream measures reviewed above and how directly each can be measured in vivo. The findings of the reviewed studies for each biomarker, by clinical phenotype, are summarized in Table 2.

Table 1. In vivo measurement of the primary pathology and of the co-pathologies encountered across the LBDS.

Target Pathology	Molecular Imaging	Fluid or Tissue Markers	Downstream Imaging and Electrophysiological Correlates	Status of In Vivo Measurement
α-Synuclein	No validated tracer. [^{18}F]ACI-12589 yields a signal in multiple system atrophy but limited retention in PD and DLB; selectivity against Aβ and tau remains unresolved.	Seed amplification assay in CSF, skin, blood and olfactory mucosa, with high diagnostic performance. Direct quantification of total, pS129 and oligomeric α-syn is non-discriminant.	Neuromelanin-sensitive MRI and nigral susceptibility; loss of dorsolateral nigral hyperintensity; nucleus basalis of Meynert volume; posterior EEG slowing; occipital hypometabolism.	Detectable but not quantifiable. Assay output is dichotomous and kinetic and quantitative readouts are still in development
Amyloid-β	Amyloid PET, with antemortem retention corresponding to Thal phase and to neuritic and total plaque burden. Positivity rises from PD-MCI through PDD to DLB.	CSF Aβ42 and, more robustly, the Aβ42/40 ratio. In blood, plasma p-tau181 and p-tau217 reflect brain amyloid status more reliably than Aβ42 itself.	Inferior-temporal volume loss; atrophy of subiculum and CA1; medial temporal hypoperfusion in the absence of a volumetric difference.	Measured directly by concordant molecular and fluid methods. Thresholds derived in AD cohorts may underestimate the burden in Lewy body disease.
Tau	Tau PET with flortaucipir, [^{18}F]PI-2620 and [^{18}F]florzolotau. Cortical uptake is low and largely conditional on amyloid presence; affinity is higher for mixed three- and four-repeat deposits.	CSF and plasma p-tau181 and p-tau217 are elevated in AD co-pathology but follow amyloid status more closely than tau PET binding (see Amyloid-β row).	Longitudinal atrophy of CA1 and subiculum; metabolic decline in the posterior cingulate with erosion of the cingulate island sign.	Measured directly, within a narrow dynamic range in this population. Non-AD tau isoforms remain unmeasured.
TDP-43	No validated tracer. The first candidate ligands are being characterized at the preclinical stage.	None specific. CSF acetylated tau-174 separates FTLD-TDP from FTLD-tau but is raised across dementia groups, DLB included.	Medial temporal atrophy and hypometabolism with relative parietal sparing; limbic atrophy exceeding what the local burden of AD pathology would predict.	Inferred rather than measured, as the fraction of medial temporal injury exceeding what amyloid and tau account for.
Cerebro-vascular	Not applicable.	Not applicable.	Primary detection rather than downstream correlate: white-matter hyperintensities and small-vessel-disease scores on structural MRI; lobar microbleeds and cortical superficial siderosis on susceptibility-weighted imaging; free-water diffusion measures.	Measured directly but not attributable to a single origin, since hypertensive and amyloid angiopathic contributions overlap.

Aβ, amyloid-β; AD, Alzheimer's disease; α-syn, α-synuclein; CA1, cornu ammonis subfield 1; CSF, cerebrospinal fluid; DLB, dementia with Lewy bodies; EEG, electroencephalography; FTLD, frontotemporal lobar degeneration; LBDS, Lewy body disease spectrum; MCI, mild cognitive impairment; MRI, magnetic resonance imaging; PD, Parkinson's disease; PD-MCI, Parkinson's disease with mild cognitive impairment; PDD, Parkinson's disease dementia; PET, positron emission tomography; p-tau, phosphorylated tau; pS129, α-synuclein phosphorylated at serine 129; TDP-43, transactive response DNA-binding protein 43 kDa.

Table 2. Findings of the reviewed studies for each biomarker across PD, PDD and DLB.

Biomarker	PD	PDD	DLB	Across the LBDS *
		α-Synuclein		
α-syn quantification in CSF and blood (total, oligomeric, pS129)	CSF total α-syn modestly reduced vs. controls, with overlapping distributions; pS129 and oligomeric species no more discriminant [26–29]. Blood levels inconsistent and confounded by hemolysis [26,30]; oligomeric α-syn accumulates in peripheral blood mononuclear cells [31].	/	CSF total α-syn not different from PD [26–28].	/
Cutaneous pS129 α-syn (immunofluorescence)	Detected in the large majority [32].	/	Detected in the large majority [32,33].	Also detected in a subset of cognitively impaired individuals without clinical DLB [33]; relationship with AD co-pathology under prospective study [34].
α-syn SAA	Positive in the large majority, with high accuracy in CSF and skin and lower sensitivity in olfactory mucosa [37]; faster seeding kinetics predict cognitive decline, also in AD-biomarker-negative patients [41].	/	Included in pooled estimates [38].	High pooled accuracy in CSF and skin; positivity criteria vary across laboratories [38]. Quantitative seed immunoassays in development [42].
Plasma strain-like α-syn species	Higher than in DLB in two independent cohorts; lower levels predict faster cognitive decline [45].	/	Lower than in PD [45].	/
α-syn PET ([^{18}F]ACI-12589)	Limited retention [19].	/	Limited retention [19].	Higher signal in SNCA duplication carriers [19,20]; binding to Aβ plaques reported in vitro [22].
		Amyloid-β		
Amyloid PET	Positivity negligible without dementia [56] and rare at the MCI stage [57]; in PD-MCI, frontal, precuneus, paracentral and putaminal deposition without grey-matter differences [64]; occipital and parietal uptake associated with lower MoCA scores [65].	Positive in a substantial proportion, with estimates varying by tracer and threshold [57,62]; regional binding matches Aβ immunohistochemistry at autopsy [55].	Positive in the majority in meta-analysis, less often in a [^{18}F]flutemetamol series [57,62]; already present at the MCI-LB stage [60]; burden increases along the DLB continuum [58,59] and with age and APOE ε4 [59,61]; retention corresponds to Thal phase and plaque burden at autopsy [53]; visual positivity predicts clinical decline [63].	Retention also scales with Braak tangle stage and LB scores [54]; positivity not accompanied by an AD-type atrophy pattern [62].
CSF Aβ42 and Aβ42/40	Low baseline Aβ42 predicts cognitive impairment in newly diagnosed PD [67] and faster decline in treated PD [68]; with high CSF NfL, predicts conversion to PDD [70]; dual SAA and Aβ42 positivity carries the fastest decline [72]; Aβ42/neurogranin ratio correlates with global cognition [71].	/	Pathological Aβ42 predicts steeper MMSE decline [69].	AD co-pathology associated with accelerated decline, higher mortality and poorer treatment response in a systematic review [10]; AD-derived thresholds may underestimate amyloid [73].

Table 2. *Cont.*

Biomarker	PD	PDD	DLB	Across the LBDS *
Plasma Aβ and p-tau	Serum/plasma Aβ42 not different from controls [77] but lower with amnestic impairment [78]; plasma p-tau217 identifies AD co-pathology [107].	/	Plasma Aβ42/40 and p-tau181/231 discriminate amyloid status without tracking decline [79]; p-tau181 and p-tau217 identify amyloid co-pathology, p-tau181 being the strongest single marker [105,106].	p-tau181 higher with intermediate or high AD neuropathologic change, unrelated to LB stage or tau PET [80]; GFAP rather than p-tau181 elevated with AD change in one series [81]; p-tau217 rises with the relative weight of the two proteinopathies [108]; in iRBD, p-tau181 with Aβ markers predicts conversion to dementia [82].
		Tau		
Tau PET	Low cortical binding without dementia; no elevation in amyloid-negative patients [85,86].	Higher than in non-demented PD, scaling with amyloid and cognition; no elevation in amyloid-negative patients [85,86].	Minimal with [^{18}F]flortaucipir [90,91]; widespread and heterogeneous with [^{18}F]florzolotau, partly AD-like [92]; occipital tau tracks local amyloid [85]; accumulates longitudinally with atrophy and decline [93]; weakly related to clinical status [96]; AD visual read positive in a minority of amyloid-positive patients [97].	[^{18}F]PI-2620 uptake low, correlated with amyloid and with executive and attention deficits [87]; baseline tau accelerates atrophy of AD-vulnerable hippocampal subfields [94].
CSF t-tau and p-tau	Unchanged or reduced vs. controls [98,99]; baseline p-tau and p-tau/Aβ42 predict memory and executive decline [100]; high p-tau/t-tau at onset predicts motor complications [101]; with Aβ42 and serum NfL, identifies the fastest decliners [102].	AD CSF signature in a substantial proportion of patients with cognitive impairment or dementia [98,99].	AD profile with elevated p-tau identifies AD co-pathology and relates to cognitive and neurodegenerative severity [83].	Antemortem t-tau/Aβ42 and Aβ42 predict cortical α-syn burden at autopsy [103].
		TDP-43		
TDP-43 (no validated in vivo marker)	/	At autopsy, explains dementia less strongly than cortical α-syn, amyloid and tau [113].	Present in a substantial minority at autopsy [110]; hippocampal TDP-43 reduces the likelihood of a clinical DLB diagnosis [112]; distinct hippocampal distribution, correlated with cognition [114]; CSF acetylated tau raised but not specific [117].	More frequent with mixed AD and Lewy pathology [111]; candidate PET ligands at the preclinical stage [115,116]; inference from disproportionate medial temporal injury relies on criteria and data from non-LBDS cohorts [118,172–174].

Table 2. *Cont.*

Biomarker	PD	PDD	DLB	Across the LBDS *
		Cerebrovascular		
Small vessel disease, microbleeds, amyloid angiopathy, free water	Greater small-vessel burden associated with worse motor impairment [121]; progression tracks cortical thinning and cognitive decline [122]; cerebral amyloid angiopathy in a minority at autopsy [124]; thalamic free water elevated and associated with glymphatic dysfunction and cognitive decline [127,128].	/	Cerebral amyloid angiopathy in the large majority at autopsy [124]; lobar microbleeds at a prevalence resembling AD, with wide variation [125]; white-matter hyperintensities correspond to AD-related change [126]; vascular burden maps to frontal, insular and thalamic atrophy [89,161].	Macroinfarcts and atherosclerosis interact with Lewy pathology to worsen parkinsonism in community-dwelling older adults [123].
		Downstream markers		
[^{123}I]FP-CIT SPECT	Caudate uptake predicts executive and visuospatial decline in de novo patients [131].	/	Distinguishes DLB from AD against autopsy, with normal scans in a minority with cortical α-syn pathology [129]; largely non-overlapping with amyloid PET at the MCI stage [60].	Normal scans more frequent in women, who carry more AD co-pathology; semiquantitative analysis improves detection [130].
Structural and susceptibility MRI	Minimal atrophy without dementia [132]; nigral neuromelanin loss [135]; nucleus basalis of Meynert volume reduced early and predicts dementia [137].	Frontal atrophy with reduced frontal coherence [133]; hippocampal atrophy at the transition from PD, pallidal volume differing from DLB [134]; regional susceptibility differs from DLB [141].	Greater hippocampal and parahippocampal loss than PD [132]; parietal atrophy with reduced posterior connectivity [133]; loss of the swallow-tail sign separates DLB from other dementias [136]; locus coeruleus neuromelanin reduced at the MCI stage [138]; regional susceptibility differs from PDD [141].	Nigral susceptibility tracks Lewy pathology at autopsy [139] and follows a prodromal-to-clinical gradient [140]; nucleus basalis volume predicts phenoconversion in iRBD [137].
MRI signatures of AD co-pathology	/	/	Amyloid maps to inferior-temporal volume loss [89]; amyloid-positive and -negative patients differ only in medial temporal hypoperfusion [163]; cortical microstructural change associated with AD co-pathology [95].	AD-type subiculum and CA1 atrophy, with baseline tau rather than amyloid driving longitudinal loss [94]; medial temporal atrophy sparing the posterior hippocampus, entorhinal volume correlating with autopsy tau [162].
Functional MRI	/	Only subtle differences from DLB [133,146].	Reduced posterior connectivity, weakly coupled to metabolism [164]; only subtle differences from PDD [133,146].	Attention and fronto-parietal hypoconnectivity and reduced network efficiency [142–145]; nucleus basalis connectivity informative for cognition [147,148]; findings vary with acquisition and analysis [149–151].

Table 2. *Cont.*

Biomarker	PD	PDD	DLB	Across the LBDS *
EEG	APOE ε4 carriers show a distinct connectivity pattern in de novo PD [165].	/	Posterior slowing of the dominant rhythm in the large majority, emerging early and correlated with fluctuations; frontal rhythmic delta activity as an adjunct [152–157]; network abnormalities already at the MCI stage [158].	/
[^{18}F]FDG PET	Hypometabolism with only marginal amyloid signal [171].	Posterior and occipital hypometabolism [160], also with only marginal amyloid signal [171].	Posterior and occipital hypometabolism with the cingulate island sign, a supportive biomarker [1,160].	Longitudinal decline parallels clinical progression [168]; cingulate island erosion tracks tau rather than amyloid [170].
NfL	Plasma NfL associated with lower cognition and predicts MMSE decline [176] and psychosis [177]; CSF NfL with low Aβ42 predicts conversion to PDD [70]; serum NfL with CSF Aβ42 and p-tau181 identifies the fastest decliners [102].	/	With GFAP, the only plasma marker retaining discriminative value in amyloid-negative DLB [106].	In iRBD, serum NfL does not track cognition and adds little to p-tau217 [178]; concentrations shift with age, body mass index and renal function in healthy individuals [179].
SV2A PET	Reduced binding largely confined to the substantia nigra without dementia [181], replicated with [^{18}F]SynVesT-1 [182].	Widespread cortical reduction, correlated with executive performance [181].	Widespread cortical reduction, correlated with executive performance [181].	Hypometabolism exceeds synaptic loss [184].
TSPO PET	Increased to a lesser extent than in PDD [171]; higher in early PD at high dementia risk, correlated with regional tau signal [187]; nigral binding predicts cognitive decline [188].	Increased in cortical and subcortical regions with only marginal amyloid signal [171].	Highest at mild stages, declining with cognitive impairment; no regional correspondence with amyloid PET [186].	/

/ = no data specific to this phenotype among the studies reviewed. * Studies reporting the LBDS as a whole, prodromal (iRBD or MCI) cohorts, or autopsy series spanning the continuum. Reviews, methodological and preclinical studies, and studies not including patients within the LBDS are not listed. Numbers refer to the reference list of the main text. Aβ, amyloid-β; AD, Alzheimer's disease; APOE, apolipoprotein E; α-syn, α-synuclein; CA1, cornu ammonis subfield 1; CSF, cerebrospinal fluid; DLB, dementia with Lewy bodies; EEG, electroencephalography; [^{18}F]FDG, 2-deoxy-2-[^{18}F]fluoro-D-glucose; [^{123}I]FP-CIT, N-ω-fluoropropyl-2β-carbomethoxy-3β-(4-[^{123}I]iodophenyl)nortropane; GFAP, glial fibrillary acidic protein; iRBD, isolated rapid eye movement sleep behavior disorder; LB, Lewy body; LBDS, Lewy body disease spectrum; MCI, mild cognitive impairment; MCI-LB, mild cognitive impairment with Lewy bodies; MMSE, Mini-Mental State Examination; MoCA, Montreal Cognitive Assessment; MRI, magnetic resonance imaging; NfL, neurofilament light chain; PD, Parkinson's disease; PDD, Parkinson's disease dementia; PET, positron emission tomography; pS129, α-synuclein phosphorylated at serine 129; p-tau, phosphorylated tau; SAA, seed amplification assay; SPECT, single-photon emission computed tomography; SV2A, synaptic vesicle glycoprotein 2A; TDP-43, transactive response DNA-binding protein 43 kDa; TSPO, 18 kDa translocator protein; t-tau, total tau.

7. Discussion

No single technique resolves the co-pathological composition of an individual along the PD–DLB continuum. Molecular and fluid assays identify protein-specific pathology but not its downstream cost, whereas structural, metabolic, and electrophysiological imaging quantify network injury but cannot attribute it to a particular protein. These approaches provide complementary information, and only their combination supports an individual proteinopathy profile in vivo.

Combining markers can improve characterization beyond that provided by any single measure [189]. α-syn SAA positivity is specific for the α-syn accumulation but silent on neurodegenerative burden, which neurofilament light supplies [190]. The same holds within imaging where dopaminergic SPECT is already informative on its own, adding a single further modality, hippocampal volume on MRI, the cingulate island ratio on [^{18}F]FDG PET, or cortical amyloid retention, improves discrimination further, and a second adds less again [191]. That evidence comes from a comparison between diagnostic groups rather than between co-pathological profiles, so it speaks to the incremental information each modality carries rather than to the performance of any profiling scheme. Applying these approaches at the individual level requires methods that quantify deviations from normative data or define disease stage over time. Normative modeling expresses a patient's structural and functional imaging as deviations from a healthy distribution, isolating where that person departs from expectation rather than from a group mean [192]. Data-driven staging adds a temporal axis. Subtype-and-stage inference applied to iRBD resolves distinct atrophy trajectories, of which a cortical-first pattern predicts progression toward DLB [193]. A quantifiable DLB-related metabolic pattern, validated across multiple centers, is elevated already at the prodromal MCI stage and rises above threshold before dementia onset while carrying an independent AD-related metabolic contribution to cognition [194]. Biological staging frameworks for LBDS offer a coordinate system into which these imaging and biomarker signatures can be mapped [195].

AD co-pathology is the most reproducible modifier of trajectory across the continuum. In a large multicenter series of patients with probable DLB classified on Aβ and tau biomarkers, close to half were amyloid positive [83], and a higher baseline amyloid burden is associated with faster grey-matter atrophy in an AD-type distribution and with faster clinical decline [196]. The prodromal DLB with AD co-pathology progresses faster than prodromal DLB without it [197]. Scalable markers make this stratification practical: plasma p-tau217 detects AD co-pathology in LBDS and predicts subsequent cognitive decline [107,198]. Biomarker-based selection is already used to enrich trial populations and match patients to mechanisms [199], and co-pathology profiling separates trajectories among patients whose clinical picture and tau burden diverge [200].

At present, the therapeutic consequences of co-pathology profiling remain narrow, as no disease-modifying treatment is approved for PD or DLB. The therapeutic reading of amyloid status is not symmetrical with the prognostic one. Amyloid-targeting antibodies are the first treatments whose eligibility rests on a co-pathology measurement, and the region of the continuum where parenchymal amyloid is most often present is also the one where its vascular form is most often present (Sections 3.1 and 5.2): cerebral amyloid angiopathy is found in the large majority of DLB, and lobar microbleeds occur at a prevalence resembling that of AD. Appropriate-use recommendations for lecanemab and for donanemab place candidates with a substantial microbleed burden, cortical superficial siderosis, or a major vascular contribution to cognitive impairment outside the treatable group. They also call for APOE genotyping before treatment, since ε4 carriers, and homozygotes in particular, carry the highest risk of amyloid-related imaging abnormalities [201,202]. The status of being an APOE ε4 carrier is simultaneously a factor influencing a positive amyloid scan in DLB

(Section 3.1), meaning that a profile pinpointing patients likely to have this co-pathology also partly highlights those for whom its removal poses the highest risk of hemorrhage. The sequences that alleviate the tension (susceptibility-weighted imaging and a microbleed count) are separate from the proteinopathy panel itself, and any precision management strategy based on amyloid status throughout this continuum must incorporate them.

A practical multimodal approach follows (Figure 1). α-syn SAA establishes the primary disease; amyloid and tau markers, in fluid or on PET, stratify the dominant co-pathology; downstream imaging and electrophysiology position the individual on axes of severity and network injury and are followed over time. Each layer answers a question the others cannot, and the composite supports a shift from a categorical PDD-versus-DLB label toward a patient-specific proteinopathic profile.

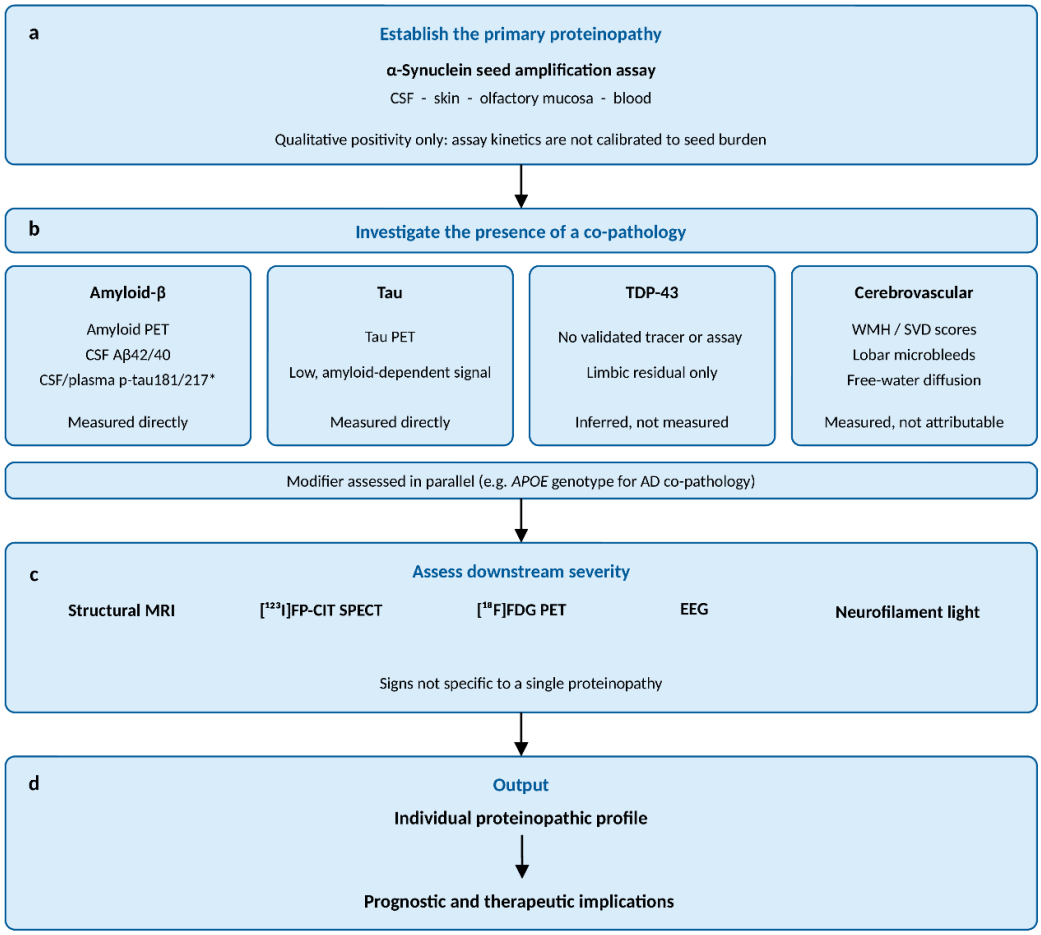


Figure 1. Multimodal approach to in vivo co-pathology profiling across the LBDS. (**a**) α-syn SAA establishes the primary proteinopathy. (**b**) Aβ and tau markers stratify the dominant co-pathology; cerebrovascular disease is measurable but not attributable to a single origin, and TDP-43 can only be inferred indirectly. (**c**) Downstream markers index disease severity without protein specificity. (**d**) Together, these layers define an individual proteinopathic profile with potential prognostic and therapeutic implications. * Soluble p-tau181 and p-tau217 are grouped with Aβ because they change early with AD neuropathologic change and, in this population, follow amyloid status more closely than tau PET binding [80,104]. Aβ, amyloid-β; *APOE*, apolipoprotein E gene; α-syn, α-synuclein; CSF, cerebrospinal fluid; EEG, electroencephalography; [^{18}F]FDG, [^{18}F]fluorodeoxyglucose; FP-CIT, *N*-ω-fluoropropyl-2β-carbomethoxy-3β-(4-iodophenyl)nortropane; LBDS, Lewy body disease spectrum; MRI, magnetic resonance imaging; PET, positron emission tomography; p-tau, phosphorylated tau; SAA, seed amplification assay; SPECT, single-photon emission computed tomography; SVD, small vessel disease; TDP-43, transactive response DNA-binding protein 43 kDa; WMH, white matter hyperintensities.

8. Conclusions and Future Directions

Across the PD–DLB continuum, some forms of co-pathology can now be measured directly, whereas others remain indirectly inferred. AD co-pathology is the most studied: amyloid is quantifiable by concordant molecular and fluid methods; tau is quantifiable with a narrow dynamic range in this population, and its non-AD forms are not. The α-syn accumulation, the hallmark, is detectable but not yet quantifiable. TDP-43 is neither and survives only as a residual once amyloid and tau are accounted for, while the cerebrovascular contribution is measurable without being attributable to a single origin. No single technique can capture the full spectrum of co-pathology, and none of the downstream signals acquires meaning until it is anchored to a molecular or fluid measure. Multimodality is therefore not simply a conceptual preference but a practical requirement: an individual proteinopathic profile exists only as the product of deliberately combined methods.

Several gaps need to be filled. First, positivity thresholds need to be defined within the LBDS rather than imported from AD cohorts: this applies to CSF Aβ42 [73], to plasma markers whose pre-defined cut-offs have not reproduced their discriminative performance in independent cohorts [106], and to SAA, whose positivity criteria still vary across laboratories [38]. Second, longitudinal cohorts with antemortem multimodal biomarkers and autopsy confirmation are required to establish which in vivo measures track the burden of each co-pathology and, in particular, to provide a first anchor for TDP-43. Third, multimodal integration schemes, including normative modeling and data-driven staging [192,193], must be validated on co-pathological profiles rather than on diagnostic groups [191], in independent cohorts and against neuropathology. Fourth, biomarker-based stratification can already inform trial design: SAA can confirm the target in α-syn-directed trials, and AD co-pathology status can be used for enrichment or as a stratification variable, given its consistent effect on the rate of decline [199]. Finally, implementation will depend on a tiered approach in which accessible blood-based and peripheral tissue markers precede CSF and PET, which remain costly and unevenly available; at the individual level, blood-based markers must be read against several physiological modifiers [179].

Looking ahead, several developments may change how we measure co-pathology. Blood-based α-syn SAA applied to neuron-derived extracellular vesicles has detected seeding activity years before the clinical diagnosis of PD in a small longitudinal series [203], and combining dermal α-syn and 4-repeat tau seed assays with serum NfL has improved discrimination among parkinsonian syndromes while revealing α-syn co-pathology [204]. Quantitative seed assays, already validated against post-mortem LB pathology load [43], may eventually supply the burden measure that current SAA lacks and serve as target-engagement readouts in α-syn-directed trials [42,205]. Artificial intelligence offers a route to integrating these heterogeneous signals. Deep learning applied to structural MRI and trained against neuropathology has yielded pathology-specific indices for AD, vascular and LB pathology [206], and machine learning applied to plasma proteomic panels [207] or to the chronology of clinical features [208] has estimated co-pathologies validated at autopsy. Performance for LB pathology nonetheless remains lower than for AD, and models trained on clinical rather than neuropathological labels risk reproducing the misclassification they aim to correct [206]. In molecular imaging, α-syn ligands with higher affinity for Lewy-type aggregates are in development [23–25], and the first TDP-43-selective tracers, [^{18}F]ACI-19626 and [^{18}F]JNJ-TDP43-1, have shown selectivity over Aβ, tau and α-syn aggregates in preclinical studies [115,209], raising the prospect that TDP-43 co-pathology may become measurable rather than inferred. Should these tools be validated, the proteinopathic profile would acquire a therapeutic role alongside its prognostic one, informing eligibility for α-syn-directed trials, the risk of amyloid-directed therapy where angiopathy co-exists, and, if TDP-43 becomes measurable, a further target for treatment.

The evidence behind these conclusions has limits. Most studies are cross-sectional and small, define groups clinically rather than at autopsy, and differ in tracers, assays, and thresholds; most cohorts come from tertiary centers. Multimodal profiling also has a cost: every added measure increases expense and patient burden and makes discordant or false-positive results more likely, and no study has yet shown that it changes outcomes. For now, in vivo co-pathology profiling is a framework for stratification and research, and its clinical value has yet to be tested prospectively.

Author Contributions: Conceptualization, D.M. and A.S.; investigation, D.M. and M.C.; writing original draft preparation, D.M.; writing/review and editing, D.M., M.C., T.S. and A.S.; visualization, D.M.; supervision, T.S. and A.S.; project administration, A.S. All authors have read and agreed to the published version of the manuscript.

Funding: This research was funded by the Italian National Institute for Insurance against Accidents at Work (INAIL) under the BRIC 2025 call to A.S. and by the European Union—NextGenerationEU through the Italian Ministry of University and Research (MUR) under PNRR-M4C2-I1.3 Project PE00000019 "Heal Italia" to T.S.

Institutional Review Board Statement: Not applicable.

Informed Consent Statement: Not applicable.

Data Availability Statement: No new datasets were created or analyzed in this study. All data discussed are available in the cited publications.

Conflicts of Interest: The authors declare no conflicts of interest.

References

1. McKeith, I.G.; Boeve, B.F.; Dickson, D.W. Diagnosis and Management of Dementia with Lewy Bodies: Fourth Consensus Report of the DLB Consortium. *Neurology* **2017**, *89*, 88–100. [CrossRef]
2. Emre, M.; Aarsland, D.; Brown, R. Clinical Diagnostic Criteria for Dementia Associated with Parkinson's Disease. *Mov. Disord.* **2007**, *22*, 1689–1707. [CrossRef]
3. Berg, D.; Postuma, R.B.; Adler, C.H. MDS Research Criteria for Prodromal Parkinson's Disease. *Mov. Disord.* **2015**, *30*, 1600–1611. [CrossRef]
4. Postuma, R.B.; Berg, D.; Stern, M.; Poewe, W.; Olanow, C.W.; Oertel, W.; Obeso, J.; Marek, K.; Litvan, I.; Lang, A.E.; et al. MDS Clinical Diagnostic Criteria for Parkinson's Disease. *Mov. Disord.* **2015**, *30*, 1591–1601. [CrossRef]
5. Outeiro, T.F.; Alcalay, R.N.; Antonini, A. Defining the Riddle in Order to Solve It: There Is More than One "Parkinson's Disease". *Mov. Disord.* **2023**, *38*, 1127–1142. [CrossRef]
6. Borghammer, P.; Okkels, N.; Weintraub, D. Parkinson's Disease and Dementia with Lewy Bodies: One and the Same. *J. Park. Dis.* **2024**, *14*, 383–397. [CrossRef]
7. Aarsland, D.; Batzu, L.; Halliday, G.M. Parkinson Disease-Associated Cognitive Impairment. *Nat. Rev. Dis. Primers* **2021**, *7*, 47. Correction in *Nat. Rev. Dis. Primers* **2021**, *7*, 53. https://doi.org/10.1038/s41572-021-00280-3. [CrossRef]
8. Toledo, J.B.; Abdelnour, C.; Weil, R.S.; Ferreira, D.; Rodriguez-Porcel, F.; Pilotto, A.; Wyman-Chick, K.A.; Grothe, M.J.; Kane, J.P.M.; Taylor, A.; et al. Dementia with Lewy Bodies: Impact of Co-pathologies and Implications for Clinical Trial Design. *Alzheimer's Dement.* **2023**, *19*, 318–332. [CrossRef]
9. Matarazzo, M. Co- and Multi-Pathologies in Parkinson's Disease: An International Parkinson and Movement Disorder Society Scientific Issues Committee Review. *Mov. Disord.* **2026**, *41*, 1979–1992. [CrossRef]
10. Tan, J.H.K.; Laurell, A.A.S.; Sidhom, E.; Rowe, J.B.; O'Brien, J.T. The Effect of Amyloid and Tau Co-Pathology on Disease Progression in Lewy Body Dementia: A Systematic Review. *Park. Relat. Disord.* **2024**, *131*, 107255. [CrossRef]
11. Simuni, T.; Chahine, L.M.; Poston, K.; Brumm, M.; Buracchio, T.; Campbell, M.; Chowdhury, S.; Coffey, C.; Concha-Marambio, L.; Dam, T.; et al. A Biological Definition of Neuronal α-Synuclein Disease: Towards an Integrated Staging System for Research. *Lancet Neurol.* **2024**, *23*, 178–190. [CrossRef]
12. Höglinger, G.U.; Adler, C.H.; Berg, D.; Klein, C.; Outeiro, T.F.; Poewe, W.; Postuma, R.; Stoessl, A.J.; Lang, A.E. A Biological Classification of Parkinson's Disease: The SynNeurGe Research Diagnostic Criteria. *Lancet Neurol.* **2024**, *23*, 191–204. Correction in *Lancet Neurol.* **2024**, *23*, E7. https://doi.org/10.1016/S1474-4422(23)00404-0. [CrossRef]

13. Reyes, N.G.D.; Pajo, A.T.; Saranza, G.; Höglinger, G.U.; Lang, A.E. Revisiting Parkinson's Disease Definition and Classification: Insights from Two Emerging Biological Frameworks. *J. Neural Transm.* **2025**, *132*, 1–15. Correction in *J. Neural Transm.* **2026**. https://doi.org/10.1007/s00702-025-03013-y. [CrossRef]
14. Mehra, S.; Sahay, S.; Maji, S.K. α-Synuclein Misfolding and Aggregation: Implications in Parkinson's Disease Pathogenesis. *Biochim. Biophys. Acta (BBA)-Proteins Proteom.* **2019**, *1867*, 890–908. [CrossRef]
15. Koga, S.; Sekiya, H.; Kondru, N.; Ross, O.A.; Dickson, D.W. Neuropathology and Molecular Diagnosis of Synucleinopathies. *Mol. Neurodegener.* **2021**, *16*, 83. [CrossRef]
16. Leak, R.K.; Clark, R.N.; Abbas, M.; Xu, F.; Brodsky, J.L.; Chen, J.; Hu, X.; Luk, K.C. Current Insights and Assumptions on α-Synuclein in Lewy Body Disease. *Acta Neuropathol.* **2024**, *148*, 18. [CrossRef]
17. Xiang, J.; Tao, Y.; Xia, Y. Development of an α-Synuclein Positron Emission Tomography Tracer for Imaging Synucleinopathies. *Cell* **2023**, *186*, 3350–3367.e19. [CrossRef]
18. Kantarci, K. Toward Imaging of Alpha-Synuclein with PET. *Cell* **2023**, *186*, 3327–3329. [CrossRef]
19. Smith, R.; Capotosti, F.; Schain, M.; Ohlsson, T.; Vokali, E.; Molette, J.; Touilloux, T.; Hliva, V.; Dimitrakopoulos, I.K.; Puschmann, A.; et al. The α-Synuclein PET Tracer [18F] ACI-12589 Distinguishes Multiple System Atrophy from Other Neurodegenerative Diseases. *Nat. Commun.* **2023**, *14*, 6750. [CrossRef]
20. Capotosti, F. A-Synuclein PET Imaging: From Clinical Utility in Multiple System Atrophy to the Possible Diagnosis of Parkinson's Disease. *Cells* **2025**, *14*, 834. [CrossRef]
21. Arias-Carrión, O.; Guerra-Crespo, M.; Padilla-Godínez, F.J.; Soto-Rojas, L.O.; Manjarrez, E. α-Synuclein Pathology in Synucleinopathies: Mechanisms, Biomarkers, and Therapeutic Challenges. *Int. J. Mol. Sci.* **2025**, *26*, 5405. [CrossRef]
22. Varlow, C.; Pees, A.; Stehouwer, J.S.; Grotegerd, A.-K.; Bleher, D.; Guarino, D.S.; Lindberg, A.; Tong, J.; Lopresti, B.J.; Knight, A.C.; et al. Autoradiography and Preclinical PET Studies with Radiolabeled Asyn-44 and ACI-12589 for Imaging α-Synuclein. *J. Park. Dis.* **2026**, *16*, 683–698. [CrossRef]
23. Korat, Š.; Bidesi, N.S.R.; Bonanno, F. Alpha-Synuclein PET Tracer Development—An Overview about Current Efforts. *Pharmaceuticals* **2021**, *14*, 847. [CrossRef]
24. Alzghool, O.M.; van Dongen, G.; van de Giessen, E.; Schoonmade, L.; Beaino, W. α-Synuclein Radiotracer Development and In Vivo Imaging: Recent Advancements and New Perspectives. *Mov. Disord.* **2022**, *37*, 936–948. [CrossRef]
25. Bidesi, N.S.R.; Vang Andersen, I.; Windhorst, A.D.; Shalgunov, V.; Herth, M.M. The Role of Neuroimaging in Parkinson's Disease. *J. Neurochem.* **2021**, *159*, 660–689. [CrossRef]
26. Barba, L.; Paolini Paoletti, F.; Bellomo, G.; Gaetani, L.; Halbgebauer, S.; Oeckl, P.; Otto, M.; Parnetti, L. Alpha and Beta Synucleins: From Pathophysiology to Clinical Application as Biomarkers. *Mov. Disord.* **2022**, *37*, 669–683. [CrossRef]
27. Eusebi, P.; Giannandrea, D.; Biscetti, L.; Abraha, I.; Chiasserini, D.; Orso, M.; Calabresi, P.; Parnetti, L. Diagnostic Utility of Cerebrospinal Fluid A-synuclein in Parkinson's Disease: A Systematic Review and Meta-analysis. *Mov. Disord.* **2017**, *32*, 1389–1400. [CrossRef]
28. Parnetti, L.; Gaetani, L.; Eusebi, P.; Paciotti, S.; Hansson, O.; El-Agnaf, O.; Mollenhauer, B.; Blennow, K.; Calabresi, P. CSF and Blood Biomarkers for Parkinson's Disease. *Lancet Neurol.* **2019**, *18*, 573–586. [CrossRef]
29. Pedersen, C.C.; Alves, G.; Tysnes, O.; Maple-Grødem, J.; Lange, J. Cerebrospinal Fluid Phosphorylated Alpha-Synuclein in Newly Diagnosed Parkinson's Disease. *Eur. J. Neurol.* **2025**, *32*, e70167. [CrossRef]
30. Barbour, R.; Kling, K.; Anderson, J.P.; Banducci, K.; Cole, T.; Diep, L.; Fox, M.; Goldstein, J.M.; Soriano, F.; Seubert, P.; et al. Red Blood Cells Are the Major Source of Alpha-Synuclein in Blood. *Neurodegener. Dis.* **2008**, *5*, 55–59. [CrossRef]
31. Veltri, F.; Sancesario, G.M.; Rosina, M.; Mascioli, D.; Bissacco, J.; Conti, M.; Zenuni, H.; Nesci, V.; Maftei, D.; Buttarazzi, V.; et al. SGK1 Downregulation Co-Occurs with Leukocyte Oligomeric α-Synuclein Accumulation in Parkinson's Disease. *Park. Relat. Disord.* **2026**, *143*, 108155. [CrossRef]
32. Gibbons, C.H. Skin Biopsy Detection of Phosphorylated Alpha-Synuclein in Patients with Synucleinopathies. *JAMA* **2024**, *331*, 1298–1306. [CrossRef]
33. Gibbons, C.H.; Levine, T.; Adler, C.H.; Bellaire, B.; Wang, N.; Agarwal, P.; Aldridge, G.M.; Barboi, A.; Claassen, D.; Evidente, V.G.H.; et al. Cutaneous Phosphorylated Alpha-Synuclein in Lewy Body Dementia. *Ann. Clin. Transl. Neurol.* **2025**, *13*, 1041–1051. [CrossRef]
34. Gibbons, C.H.; Galasko, D.; Press, D.; Claassen, D.; Levine, T.; Freeman, R. The Syn-D Study: Detection of Cutaneous Phosphorylated Alpha-Synuclein in Mild Cognitive Impairment a Trial Protocol. *Biomark. Med.* **2025**, *19*, 501–508. [CrossRef]
35. Huang, J.; Yuan, X.; Chen, L.; Hu, B.; Wang, H.; Wang, Y.; Huang, W. Pathological α-Synuclein Detected by Real-Time Quaking-Induced Conversion in Synucleinopathies. *Exp. Gerontol.* **2024**, *187*, 112366. [CrossRef]
36. Srivastava, A.; Alam, P.; Caughey, B. RT-QuIC and Related Assays for Detecting and Quantifying Prion-like Pathological Seeds of α-Synuclein. *Biomolecules* **2022**, *12*, 576. [CrossRef]
37. Rissardo, J.P.; Fornari Caprara, A.L. Alpha-Synuclein Seed Amplification Assays in Parkinson's Disease: A Systematic Review and Network Meta-Analysis. *Clin. Pract.* **2025**, *15*, 107. [CrossRef]

38. Helbling, C.; Yeung, S.; DeMarco, M.L. α-Synuclein Seed Amplification Assay Methodology and Performance in Parkinson's Disease, Lewy Body Dementia, and Multiple System Atrophy: A Meta-Analysis. *Clin. Biochem.* **2026**, *142*, 111093. [CrossRef]
39. Parveen, S.; Alam, P.; Orrù, C.D. A Same Day α-Synuclein RT-QuIC Seed Amplification Assay for Synucleinopathy Biospecimens. *npj Biosens.* **2025**, *2*, 8. [CrossRef]
40. Painous, C.; Fernández, M.; Pérez, J.; de Mena, L.; Cámara, A.; Compta, Y. Fluid and Tissue Biomarkers in Parkinson's Disease: Immunodetection or Seed Amplification? Central or Peripheral? *Park. Relat. Disord.* **2023**, *121*, 105968. [CrossRef]
41. Orrú, C.D.; Vaughan, D.P.; Vijiaratnam, N.; Real, R.; Martinez-Carrasco, A.; Fumi, R.; Jensen, M.T.; Hodgson, M.; Girges, C.; Gil-Martinez, A.-L.; et al. Diagnostic and Prognostic Value of α-Synuclein Seed Amplification Assay Kinetic Measures in Parkinson's Disease: A Longitudinal Cohort Study. *Lancet Neurol.* **2025**, *24*, 580–590. [CrossRef]
42. Abdi, I.Y.; Sudhakaran, I.P.; Ghanem, S.S.; Vaikath, N.N.; Majbour, N.; Goh, Y.Y.; Vijiaratnam, N.; Girges, C.; Constantinides, V.C.; Kapaki, E.; et al. Quantitative Measurements of α-Synuclein Seeds in CSF Inform Diagnosis of Synucleinopathies. *J. Park. Dis.* **2025**, *15*, 1412–1430. [CrossRef]
43. Mastrangelo, A.; Caldera, S.; Mastenbroek, S.E.; Vittoriosi, E.; Janelidze, S.; Serrano, G.E.; Atri, A.; Shill, H.; Driver-Dunckley, E.; Mehta, S.; et al. Quantification of Lewy Body Pathology by Cerebrospinal Fluid Endpoint Dilution RT-QuIC in a Neuropathological Autopsy Cohort of Clinically Heterogeneous Participants. *Acta Neuropathol.* **2025**, *149*, 67. [CrossRef]
44. Silva-Rodríguez, J.; Labrador-Espinosa, M.A.; Zhang, L. The Effect of Lewy Body (Co-)Pathology on the Clinical and Imaging Phenotype of Amnestic Patients. *Brain* **2025**, *148*, 2441–2452. [CrossRef]
45. Kannarkat, G.T. Blood α-Synuclein Separates Parkinson's Disease from Dementia with Lewy Bodies. *Ann. Neurol.* **2025**, *98*, 682–698. [CrossRef]
46. Raina, A.; Wang, W.; Gonzalez, J.C.; Yan, X.; Overstreet-Wadiche, L.; Wadiche, J.I.; Zhang, C.-L.; Chen, S.G. Skin-Derived α-Synuclein Strains from PD, DLB, and MSA Induce Distinct Intracellular Pathology and Neurodegeneration. *J. Biol. Chem.* **2025**, *302*, 111005. [CrossRef]
47. Kaya, Z.B.; Amerna, D.; Susarla, A.; Lim, M.J.; Bregendahl, M.; Sekiya, H.; DeTure, M.; Ross, O.A.; Dickson, D.W.; Boschen, S.L.; et al. Molecular Profiling of Alpha-Synuclein Pathology and Seeding Activity in Parkinson's Disease. *Acta Neuropathol.* **2026**, *151*, 54. [CrossRef]
48. Trejo-Lopez, J.A.; Yachnis, A.T.; Prokop, S. Neuropathology of Alzheimer's Disease. *Neurotherapeutics* **2022**, *19*, 173–185. [CrossRef]
49. Sengupta, U.; Kayed, R. Amyloid β, Tau, and α-Synuclein Aggregates in the Pathogenesis, Prognosis, and Therapeutics for Neurodegenerative Diseases. *Prog. Neurobiol.* **2022**, *214*, 102270. [CrossRef]
50. Chen, L.; Lu, H.; Mao, L.; Lin, J.; Liu, P. Unraveling the Interplay of β-Amyloid Pathology and Parkinson's Disease Progression: Insights from Autopsy-Confirmed Patients. *Heliyon* **2024**, *10*, e39194. [CrossRef]
51. Villemagne, V.L.; Doré, V.; Burnham, S.C.; Masters, C.L.; Rowe, C.C. Imaging Tau and Amyloid-β Proteinopathies in Alzheimer Disease and Other Conditions. *Nat. Rev. Neurol.* **2018**, *14*, 225–236. Correction in *Nat. Rev. Neurol.* **2018**, *14*, 446. https://doi.org/10.1038/nrneurol.2018.9. [CrossRef]
52. Klunk, W.E.; Engler, H.; Nordberg, A.; Wang, Y.; Blomqvist, G.; Holt, D.P.; Bergström, M.; Savitcheva, I.; Huang, G.; Estrada, S.; et al. Imaging Brain Amyloid in Alzheimer's Disease with Pittsburgh Compound-B. *Ann. Neurol.* **2004**, *55*, 306–319. [CrossRef]
53. Kantarci, K.; Lowe, V.J.; Chen, Q.; Przybelski, S.A.; Lesnick, T.G.; Schwarz, C.G.; Senjem, M.L.; Gunter, J.L.; Jack, C.R.; Graff-Radford, J.; et al. β-Amyloid PET and Neuropathology in Dementia with Lewy Bodies. *Neurology* **2020**, *94*, e282–e291. [CrossRef]
54. Shirvan, J.; Clement, N.; Ye, R.; Katz, S.; Schultz, A.; Johnson, K.A.; Gomez-Isla, T.; Frosch, M.; Growdon, J.H.; Gomperts, S.N. Neuropathologic Correlates of Amyloid and Dopamine Transporter Imaging in Lewy Body Disease. *Neurology* **2019**, *93*, e476–e484. [CrossRef]
55. Akhtar, R.S.; Xie, S.X.; Brennan, L.; Pontecorvo, M.J.; Hurtig, H.I.; Trojanowski, J.Q.; Weintraub, D.; Siderowf, A.D. Amyloid-Beta Positron Emission Tomography Imaging of Alzheimer's Pathology in Parkinson's Disease Dementia. *Mov. Disord. Clin. Pract.* **2016**, *3*, 367–375. [CrossRef]
56. Mashima, K.; Ito, D.; Kameyama, M.; Osada, T.; Tabuchi, H.; Nihei, Y.; Yoshizaki, T.; Noguchi, E.; Tanikawa, M.; Iizuka, T.; et al. Extremely Low Prevalence of Amyloid Positron Emission Tomography Positivity in Parkinson's Disease without Dementia. *Eur. Neurol.* **2017**, *77*, 231–237. [CrossRef]
57. Petrou, M.; Dwamena, B.A.; Foerster, B.R.; MacEachern, M.P.; Bohnen, N.I.; Müller, M.L.; Albin, R.L.; Frey, K.A. Amyloid Deposition in Parkinson's Disease and Cognitive Impairment: A Systematic Review. *Mov. Disord.* **2015**, *30*, 928–935. [CrossRef]
58. Donaghy, P.; Thomas, A.J.; O'Brien, J.T. Amyloid PET Imaging in Lewy Body Disorders. *Am. J. Geriatr. Psychiatry* **2015**, *23*, 23–37. [CrossRef]
59. Diaz-Galvan, P.; Przybelski, S.A.; Lesnick, T.G.; Schwarz, C.G.; Senjem, M.L.; Gunter, J.L.; Jack, C.R.; Min, H.-K.P.; Jain, M.; Miyagawa, T.; et al. β-Amyloid Load on PET Along the Continuum of Dementia with Lewy Bodies. *Neurology* **2023**, *101*, e178–e188. [CrossRef]

60. Chen, Q.; Lowe, V.J.; Boeve, B.F.; Przybelski, S.A.; Miyagawa, T.; Senjem, M.L.; Jack, C.R.; Lesnick, T.G.; Kremers, W.K.; Fields, J.A.; et al. β-Amyloid PET and ^{123} I-FP-CIT SPECT in Mild Cognitive Impairment at Risk for Lewy Body Dementia. *Neurology* **2021**, *96*, e1180–e1189. [CrossRef]
61. Ossenkoppele, R.; Jansen, W.J.; Rabinovici, G.D.; Knol, D.L.; van der Flier, W.M.; van Berckel, B.N.M.; Scheltens, P.; Visser, P.J.; Verfaillie, S.C.J.; Zwan, M.D.; et al. Prevalence of Amyloid PET Positivity in Dementia Syndromes. *JAMA* **2015**, *313*, 1939. [CrossRef]
62. Biundo, R.; Weis, L.; Fiorenzato, E.; Pistonesi, F.; Cagnin, A.; Bertoldo, A.; Anglani, M.; Cecchin, D.; Antonini, A. The Contribution of Beta-Amyloid to Dementia in Lewy Body Diseases: A 1-Year Follow-up Study. *Brain Commun.* **2021**, *3*, fcab180. [CrossRef]
63. Donaghy, P.C.; Firbank, M.J.; Thomas, A.J.; Lloyd, J.; Petrides, G.; Barnett, N.; Olsen, K.; O'Brien, J.T. Amyloid Imaging and Longitudinal Clinical Progression in Dementia with Lewy Bodies. *Am. J. Geriatr. Psychiatry* **2020**, *28*, 573–577. [CrossRef]
64. Garon, M.; Weis, L.; Fiorenzato, E.; Pistonesi, F.; Cagnin, A.; Bertoldo, A.; Anglani, M.; Cecchin, D.; Antonini, A.; Biundo, R. Quantification of Brain β-Amyloid Load in Parkinson's Disease with Mild Cognitive Impairment: A PET/MRI Study. *Front. Neurol.* **2022**, *12*, 760518. [CrossRef]
65. Mihaescu, A.S.; Valli, M.; Uribe, C.; Diez-Cirarda, M.; Masellis, M.; Graff-Guerrero, A.; Strafella, A.P. Beta Amyloid Deposition and Cognitive Decline in Parkinson's Disease: A Study of the PPMI Cohort. *Mol. Brain* **2022**, *15*, 79. [CrossRef]
66. Amft, M.; Ortner, M.; Eichenlaub, U.; Goldhardt, O.; Diehl-Schmid, J.; Hedderich, D.M.; Yakushev, I.; Grimmer, T. The Cerebrospinal Fluid Biomarker Ratio Aβ42/40 Identifies Amyloid Positron Emission Tomography Positivity Better than Aβ42 Alone in a Heterogeneous Memory Clinic Cohort. *Alzheimer's Res. Ther.* **2022**, *14*, 60. [CrossRef]
67. Terrelonge, M.; Marder, K.S.; Weintraub, D.; Alcalay, R.N. CSF β-Amyloid 1-42 Predicts Progression to Cognitive Impairment in Newly Diagnosed Parkinson Disease. *J. Mol. Neurosci.* **2016**, *58*, 88–92. [CrossRef]
68. Siderowf, A.; Xie, S.X.; Hurtig, H.; Weintraub, D.; Duda, J.; Chen-Plotkin, A.; Shaw, L.M.; Van Deerlin, V.; Trojanowski, J.Q.; Clark, C. CSF Amyloid β 1-42 Predicts Cognitive Decline in Parkinson Disease. *Neurology* **2010**, *75*, 1055–1061. [CrossRef]
69. Abdelnour, C.; van Steenoven, I.; Londos, E.; Blanc, F.; Auestad, B.; Kramberger, M.G.; Zetterberg, H.; Mollenhauer, B.; Boada, M.; Aarsland, D. Alzheimer's Disease Cerebrospinal Fluid Biomarkers Predict Cognitive Decline in Lewy Body Dementia. *Mov. Disord.* **2016**, *31*, 1203–1208. Correction in *Mov. Disord.* **2019**, *34*, 593. https://doi.org/10.1002/mds.26668. [CrossRef]
70. Bäckström, D.; Granåsen, G.; Mo, S.J.; Riklund, K.; Trupp, M.; Zetterberg, H.; Blennow, K.; Forsgren, L.; Domellöf, M.E. Prediction and Early Biomarkers of Cognitive Decline in Parkinson Disease and Atypical Parkinsonism: A Population-Based Study. *Brain Commun.* **2022**, *4*, fcac040. [CrossRef]
71. Sancesario, G.M.; Di Lazzaro, G.; Alwardat, M.; Biticchi, B.; Basile, V.; Salimei, C.; Colona, V.L.; Sinibaldi Salimei, P.; Bernardini, S.; Mercuri, N.B.; et al. Amyloid-B42/Neurogranin Ratio as a Potential Index for Cognitive Impairment in Parkinson's Disease. *J. Alzheimer's Dis.* **2020**, *76*, 1171–1178. [CrossRef]
72. Qiang, Q.; Skudder-Hill, L.; Toyota, T.; Huang, Z.; Wei, W.; Adachi, H. Combination of CSF α-Synuclein Seed Amplification Assay and Amyloid-B42 Predicts Cognitive Decline in Parkinson's Disease. *Neurobiol. Dis.* **2026**, *225*, 107452. [CrossRef]
73. Irwin, D.J.; Fedler, J.; Coffey, C.S.; Caspell-Garcia, C.; Kang, J.H.; Simuni, T.; Foroud, T.; Toga, A.W.; Tanner, C.M.; Kieburtz, K.; et al. Evolution of Alzheimer's Disease Cerebrospinal Fluid Biomarkers in Early Parkinson's Disease. *Ann. Neurol.* **2020**, *88*, 574–587. [CrossRef]
74. Bousiges, O.; Cretin, B.; Battista, L.; Schaefer-Agalède, C.; Philippi, N.; Hamied, L.; Ravier, A.; Demuynck, C.; Muller, C.; Blanc, F. CSF Elevated Tau and P-Tau and Normal Aβ42 Mainly Corresponds to Alzheimer's Disease with Dementia with Lewy Bodies. *Geroscience* **2026**, *48*, 1–15. [CrossRef]
75. Barthélemy, N.R.; Salvadó, G.; Schindler, S.E.; He, Y.; Janelidze, S.; Collij, L.E.; Saef, B.; Henson, R.L.; Chen, C.D.; Gordon, B.A.; et al. Highly Accurate Blood Test for Alzheimer's Disease Is Similar or Superior to Clinical Cerebrospinal Fluid Tests. *Nat. Med.* **2024**, *30*, 1085–1095. [CrossRef]
76. Mattsson-Carlgren, N.; Karlsson, L.; Tang, W.; Blennow, K.; Zetterberg, H.; Bateman, R.J.; Schindler, S.E.; Barthelemy, N.; Palmqvist, S.; Stomrud, E.; et al. Prediction of Continuous Amyloid Positron Emission Tomography with Fluid Measures of Phosphorylated Tau and β-Amyloid. *EMBO Mol. Med.* **2025**, *18*, 217–231. [CrossRef]
77. Schirinzi, T.; Zenuni, H.; Grillo, P.; Bovenzi, R.; Guerrera, G.; Gargano, F.; Pieri, M.; Bernardini, S.; Biagio Mercuri, N.; Battistini, L.; et al. Tau and Amyloid-β Peptides in Serum of Patients with Parkinson's Disease: Correlations with CSF Levels and Clinical Parameters. *Front. Neurol.* **2022**, *13*, 748599. [CrossRef]
78. Xue, X.; Mei, S.; Huang, A.; Wu, Z.; Zeng, J.; Song, H.; An, J.; Zhang, L.; Liu, G.; Zhou, L.; et al. Alzheimer's Disease Related Biomarkers Were Associated with Amnestic Cognitive Impairment in Parkinson's Disease: A Cross-Sectional Cohort Study. *Brain Sci.* **2024**, *14*, 787. [CrossRef]
79. Bolsewig, K.; van Unnik, A.A.J.M.; Blujdea, E.R.; Gonzalez, M.C.; Ashton, N.J.; Aarsland, D.; Zetterberg, H.; Padovani, A.; Bonanni, L.; Mollenhauer, B.; et al. Association of Plasma Amyloid, P-Tau, GFAP, and NfL with CSF, Clinical, and Cognitive Features in Patients with Dementia with Lewy Bodies. *Neurology* **2024**, *102*, e209418. [CrossRef]

80. Ye, R.; Kivisäkk, P.; Goodheart, A.; Fatima, H.; Peterec, E.; Thibault, E.; Properzi, M.; Johnson, K.; Arnold, S.; Gomperts, S.N. Plasma Phosphorylated Tau181 as a Biomarker for Alzheimer's Disease Co-Pathology in Lewy Body Disease. *Mov. Disord.* **2025**, *40*, 1930–1939. [CrossRef]
81. Cousins, K.A.Q.; Irwin, D.J.; Chen-Plotkin, A.; Shaw, L.M.; Arezoumandan, S.; Lee, E.B.; Wolk, D.A.; Weintraub, D.; Spindler, M.; Deik, A.; et al. Plasma GFAP Associates with Secondary Alzheimer's Pathology in Lewy Body Disease. *Ann. Clin. Transl. Neurol.* **2023**, *10*, 802–813. [CrossRef]
82. Delva, A.; Pelletier, A.; Somerville, E.; Montplaisir, J.; Gagnon, J.-F.; Kollmorgen, G.; Kam-Thong, T.; Kustermann, T.; Machado, V.; Gan-Or, Z.; et al. Plasma PTau181 and Amyloid Markers Predict Conversion to Dementia in Idiopathic REM Sleep Behaviour Disorder. *Brain* **2025**, *148*, 2049–2059. [CrossRef]
83. Ferreira, D.; Przybelski, S.A.; Lesnick, T.G.; Lemstra, A.W.; Londos, E.; Blanc, F.; Nedelska, Z.; Schwarz, C.G.; Graff-Radford, J.; Senjem, M.L.; et al. β-Amyloid and Tau Biomarkers and Clinical Phenotype in Dementia with Lewy Bodies. *Neurology* **2020**, *95*, e3257–e3268. [CrossRef]
84. Avila, J. Tau Phosphorylation and Aggregation in Alzheimer's Disease Pathology. *FEBS Lett.* **2006**, *580*, 2922–2927. [CrossRef]
85. Lee, S.H.; Cho, H.; Choi, J.Y.; Lee, J.H.; Ryu, Y.H.; Lee, M.S.; Lyoo, C.H. Distinct Patterns of Amyloid-Dependent Tau Accumulation in Lewy Body Diseases. *Mov. Disord.* **2018**, *33*, 262–272. [CrossRef]
86. Gomperts, S.N.; Locascio, J.J.; Makaretz, S.J.; Schultz, A.; Caso, C.; Vasdev, N.; Sperling, R.; Growdon, J.H.; Dickerson, B.C.; Johnson, K. Tau Positron Emission Tomographic Imaging in the Lewy Body Diseases. *JAMA Neurol.* **2016**, *73*, 1334–1341. [CrossRef]
87. Winer, J.R.; Vossler, H.; Young, C.B.; Smith, V.; Romero, A.; Shahid-Besanti, M.; Abdelnour, C.; Wilson, E.N.; Mormino, E.C.; Poston, K.L. 18F-PI-2620 Tau PET Is Associated with Cognitive and Motor Impairment in Lewy Body Disease. *Brain Commun.* **2024**, *7*, fcae458. [CrossRef]
88. Lowe, V.J.; Curran, G.; Fang, P.; Liesinger, A.M.; Josephs, K.A.; Parisi, J.E. An Autoradiographic Evaluation of AV-1451 Tau PET in Dementia. *Acta Neuropathol. Commun.* **2016**, *4*, 58. [CrossRef]
89. Ferreira, D. Cross-Sectional Associations of β-Amyloid, Tau, and Cerebrovascular Biomarkers with Neurodegeneration in Probable Dementia with Lewy Bodies. *Neurology* **2022**, *100*, e846–e859. [CrossRef]
90. Mak, E.; Nicastro, N.; Malpetti, M. Imaging Tau Burden in Dementia with Lewy Bodies Using [18F]-AV1451 Positron Emission Tomography. *Neurobiol. Aging* **2021**, *101*, 172–180. [CrossRef]
91. Smith, R. 18F-AV-1451 in Parkinson's Disease with and without Dementia and in Dementia with Lewy Bodies. *Sci. Rep.* **2018**, *8*, 4717. [CrossRef]
92. Tang, G.; Lu, J.; Li, X.; Yao, R.; Yang, Y.; Jiao, F.; Chen, M.; Liang, X.; Ju, Z.; Ge, J.; et al. ^{18}F-Florzolotau PET Imaging Unveils Tau Pathology in Dementia with Lewy Bodies. *Mov. Disord.* **2025**, *40*, 108–120. [CrossRef]
93. Chen, Q. Longitudinal Tau PET in Dementia with Lewy Bodies. *Mov. Disord.* **2022**, *37*, 1256–1264. [CrossRef]
94. Ye, R.; Goodheart, A.E.; Locascio, J.J.; Peterec, E.; Properzi, M.; Thibault, E.G.; Chuba, E.; Johnson, K.A.; Brickhouse, M.J.; Touroutoglou, A.; et al. Differential Vulnerability of Hippocampal Subfields to Amyloid and Tau Deposition in the Lewy Body Diseases. *Neurology* **2024**, *102*, e209460. [CrossRef]
95. Mak, E. Cortical Microstructural Abnormalities in Dementia with Lewy Bodies and Their Associations with Alzheimer's Disease Copathologies. *npj Park. Dis.* **2025**, *11*, 124. Correction in *npj Park. Dis.* **2025**, *11*, 209. https://doi.org/10.1038/s41531-025-00944-x. [CrossRef]
96. Wolters, E.E. Tau PET and Relative Cerebral Blood Flow in Dementia with Lewy Bodies: A PET Study. *NeuroImage Clin.* **2020**, *28*, 102504. [CrossRef]
97. Coomans, E.M. Interobserver Agreement and Clinical Utility of Flortaucipir Visual Assessment across the Alzheimer Disease Continuum and in Dementia with Lewy Bodies. *Neurology* **2023**, *101*, e1850–e1862. Correction in *Neurology* **2023**, *103*, e209596. https://doi.org/10.1212/WNL.0000000000207794.
98. Montine, T.J.; Shi, M.; Quinn, J.F.; Peskind, E.R.; Craft, S.; Ginghina, C.; Chung, K.A.; Kim, H.; Galasko, D.R.; Jankovic, J.; et al. CSF Aβ42 and Tau in Parkinson's Disease with Cognitive Impairment. *Mov. Disord.* **2010**, *25*, 2682–2685. [CrossRef]
99. Mollenhauer, B.; Caspell-Garcia, C.J.; Coffey, C.S.; Taylor, P.; Shaw, L.M.; Trojanowski, J.Q.; Singleton, A.; Frasier, M.; Marek, K.; Galasko, D. Longitudinal CSF Biomarkers in Patients with Early Parkinson Disease and Healthy Controls. *Neurology* **2017**, *89*, 1959–1969. [CrossRef]
100. Liu, C.; Cholerton, B.; Shi, M.; Ginghina, C.; Cain, K.C.; Auinger, P.; Zhang, J. CSF Tau and Tau/Aβ42 Predict Cognitive Decline in Parkinson's Disease. *Park. Relat. Disord.* **2015**, *21*, 271–276. [CrossRef]
101. Bissacco, J.; Di Lazzaro, G.; Bovenzi, R.; Sancesario, G.M.; Conti, M.; Simonetta, C.; Mascioli, D.; Mancini, M.; Buttarazzi, V.; Pierantozzi, M.; et al. CSF Phospho-Tau Levels at Parkinson's Disease Onset Predict the Risk for Development of Motor Complications. *J. Neurol.* **2025**, *272*, 573. [CrossRef]

102. Cousins, K.A.Q.; Irwin, D.J.; Tropea, T.F.; Rhodes, E.; Phillips, J.; Chen-Plotkin, A.S.; Brumm, M.C.; Coffey, C.S.; Kang, J.H.; Simuni, T.; et al. Evaluation of ATN_{PD} Framework and Biofluid Markers to Predict Cognitive Decline in Early Parkinson Disease. *Neurology* **2024**, *102*, e208033. [CrossRef]
103. Irwin, D.J.; Xie, S.X.; Coughlin, D.; Nevler, N.; Akhtar, R.S.; McMillan, C.T.; Lee, E.B.; Wolk, D.A.; Weintraub, D.; Chen-Plotkin, A.; et al. CSF Tau and β-Amyloid Predict Cerebral Synucleinopathy in Autopsied Lewy Body Disorders. *Neurology* **2018**, *90*, e1038–e1046. [CrossRef]
104. Jack, C.R.; Andrews, J.S.; Beach, T.G.; Buracchio, T.; Dunn, B.; Graf, A.; Hansson, O.; Ho, C.; Jagust, W.; McDade, E.; et al. Revised Criteria for Diagnosis and Staging of Alzheimer's Disease: Alzheimer's Association Workgroup. *Alzheimer's Dement.* **2024**, *20*, 5143–5169. [CrossRef]
105. Jiao, B. Evaluating the Diagnostic Performance of Six Plasma Biomarkers for Alzheimer's Disease and Other Neurodegenerative Dementias in a Large Chinese Cohort. *Alzheimer's Res. Ther.* **2025**, *17*, 71. [CrossRef]
106. Doecke, J.D. Diagnostic Performance of Plasma Aβ42/40 Ratio, p-Tau181, GFAP, and NfL along the Continuum of Alzheimer's Disease and Non-AD Dementias. *Alzheimer's Dement.* **2025**, *21*, e14573. [CrossRef]
107. Tropea, T.; Stevenson, P.; Flitter, M.; Meehan, D.; Morris, A.; Lu, M.; Iaccarino, L.; Collins, E.; Hodsdon, M.; Irwin, D.; et al. Association between Plasma P-tau217 and Alzheimer's Copathology and Cognitive Decline in Parkinson's Disease. *Ann. Neurol.* **2026**, *99*, 1428–1437. [CrossRef]
108. Tort-Merino, A.; Esteller-Gauxax, D.; Pérez-Millan, A.; Castellví, M.; Bosch, B.; Sánchez-Rodríguez, M.M.; Rigol, A.; Rubio, G.; Morante-Serra, C.; Mir-Sala, L.; et al. Neuropsychological Profile and Cognitive Trajectories of Patients with Biomarker Evidence of Alzheimer Disease or Dementia with Lewy Bodies. *Neurology* **2026**, *107*, e218201. [CrossRef]
109. de Boer, E.M.J.; Orie, V.K.; Williams, T.; Baker, M.R.; De Oliveira, H.M.; Polvikoski, T.; Silsby, M.; Menon, P.; van den Bos, M.; Halliday, G.M.; et al. TDP-43 Proteinopathies: A New Wave of Neurodegenerative Diseases. *J. Neurol. Neurosurg. Psychiatry* **2021**, *92*, 86–95. [CrossRef]
110. McAleese, K.E.; Walker, L.; Erskine, D.; Thomas, A.J.; McKeith, I.G.; Attems, J. TDP-43 Pathology in Alzheimer's Disease, Dementia with Lewy Bodies and Ageing. *Brain Pathol.* **2017**, *27*, 472–479. [CrossRef]
111. Robinson, J.L.; Xie, S.X.; Baer, D.R.; Suh, E.; Van Deerlin, V.M.; Loh, N.J.; Irwin, D.J.; McMillan, C.T.; Wolk, D.A.; Chen-Plotkin, A.; et al. Pathological Combinations in Neurodegenerative Disease Are Heterogeneous and Disease-Associated. *Brain* **2023**, *146*, 2557–2569. [CrossRef]
112. Buciuc, M. TDP-43 Is Associated with a Reduced Likelihood of Rendering a Clinical Diagnosis of Dementia with Lewy Bodies in Autopsy-Confirmed Cases of Transitional/Diffuse Lewy Body Disease. *J. Neurol.* **2020**, *267*, 1444–1453. [CrossRef]
113. Smith, C.; Malek, N.; Grosset, K.; Cullen, B.; Gentleman, S.; Grosset, D.G. Neuropathology of Dementia in Patients with Parkinson's Disease: A Systematic Review of Autopsy Studies. *J. Neurol. Neurosurg. Psychiatry* **2019**, *90*, 1234–1243. [CrossRef]
114. Uemura, M.T.; Robinson, J.L.; Cousins, K.A.Q.; Tropea, T.F.; Kargilis, D.C.; McBride, J.D.; Suh, E.; Xie, S.X.; Xu, Y.; Porta, S.; et al. Distinct Characteristics of Limbic-Predominant Age-Related TDP-43 Encephalopathy in Lewy Body Disease. *Acta Neuropathol.* **2022**, *143*, 15–31. [CrossRef]
115. Irwin, D.J. The Potential of TDP-43 PET Ligands for a Biological Diagnosis of TDP-43 Proteinopathies. *Nat. Commun.* **2025**, *16*, 9357. [CrossRef]
116. Vokali, E.; Chevalier, E.; Dreyfus, N.; Charmey, D.; Melly, T.; Kocher, J.; Ratnam, M.; Serra, A.M.; Jaquier, T.; Delgado, C.; et al. Development of [18F]ACI-19626 as a First-in-Class Brain PET Tracer for Imaging TDP-43 Pathology. *Nat. Commun.* **2025**, *16*, 9358. [CrossRef]
117. Honey, M.I.J.; Hok-A-Hin, Y.S.; Thijssen, E.H.; Cousins, K.A.Q.; van der Weijden, B.; In't Veld, L.; Stoops, E.; de Boer, S.C.M.; Duits, F.H.; de Houwer, J.F.H.; et al. An Acetylated Tau-174 CSF Biomarker Discriminates between TDP-43 and Tau Pathology in Patients with Frontotemporal Lobar Degeneration. *Nat. Med.* **2026**, *32*, 2083–2095. [CrossRef]
118. Wolk, D.A. Clinical Criteria for Limbic-Predominant Age-Related TDP-43 Encephalopathy. *Alzheimer's Dement.* **2025**, *21*, e14202. [CrossRef]
119. Torso, M. In Vivo Cortical Diffusion Imaging Relates to Alzheimer's Disease Neuropathology. *Alzheimer's Res. Ther.* **2023**, *15*, 165. [CrossRef]
120. Markus, H.S. Cerebral Small Vessel Disease: Recent Advances and Future Directions. *Int. J. Stroke* **2023**, *18*, 4–14. [CrossRef]
121. Wan, Y. Exploring the Association between Cerebral Small-Vessel Diseases and Motor Symptoms in Parkinson's Disease. *Brain Behav.* **2019**, *9*, e01219. [CrossRef]
122. Foo, H. Progression of Small Vessel Disease Correlates with Cortical Thinning in Parkinson's Disease. *Park. Relat. Disord.* **2016**, *31*, 34–40. [CrossRef]
123. Agrawal, S.; Leurgans, S.E.; Nag, S.; Oveisgharan, S.; Barnes, L.L.; Bennett, D.A.; Buchman, A.S.; Schneider, J.A. Effects of Cerebrovascular and Lewy Body Pathology on Parkinsonian Signs in Community-Dwelling Older Adults. *Neurology* **2023**, *101*, e754–e763. [CrossRef]

124. Jellinger, K.A. Significance of Cerebral Amyloid Angiopathy and Other Co-Morbidities in Lewy Body Diseases. *J. Neural Transm.* **2021**, *128*, 687–699. [CrossRef]
125. Hijazi, Z.; Yassi, N.; O'Brien, J.T.; Watson, R. The Influence of Cerebrovascular Disease in Dementia with Lewy Bodies and Parkinson's Disease Dementia. *Eur. J. Neurol.* **2022**, *29*, 1254–1265. [CrossRef]
126. Joki, H.; Higashiyama, Y.; Nakae, Y.; Kugimoto, C.; Doi, H.; Kimura, K.; Kishida, H.; Ueda, N.; Nakano, T.; Takahashi, T.; et al. White Matter Hyperintensities on MRI in Dementia with Lewy Bodies, Parkinson's Disease with Dementia, and Alzheimer's Disease. *J. Neurol. Sci.* **2018**, *385*, 99–104. [CrossRef]
127. Kuang, Z.; Huang, X.; Wang, M. Thalamic Free Water Elevation and Its Association with Glymphatic Dysfunction in Parkinson's Disease: A Cross-Sectional and Longitudinal Study. *Neuroscience* **2025**, *579*, 218–226. [CrossRef]
128. Guttuso, T.; Sirica, D.; Tosun, D.; Zivadinov, R.; Pasternak, O.; Weintraub, D.; Baglio, F.; Bergsland, N. Thalamic Dorsomedial Nucleus Free Water Correlates with Cognitive Decline in Parkinson's Disease. *Mov. Disord.* **2022**, *37*, 490–501. [CrossRef]
129. Thomas, A.J.; Attems, J.; Colloby, S.J.; O'Brien, J.T.; McKeith, I.; Walker, R.; Lee, L.; Burn, D.; Lett, D.J.; Walker, Z. Autopsy Validation of ^{123}I-FP-CIT Dopaminergic Neuroimaging for the Diagnosis of DLB. *Neurology* **2017**, *88*, 276–283. [CrossRef]
130. Miyagawa, T.; Przybelski, S.A.; Vernon, C.J.; Paul Min, H.-K.; Forsberg, L.K.; Fields, J.A.; McCarter, S.J.; Ferman, T.J.; Ramanan, V.K.; Graff-Radford, J.; et al. ^{123}I-FP-CIT SPECT in Autopsy-Proven Lewy Body Disease. *Neurol. Open Access* **2025**, *1*, e000048. [CrossRef]
131. Arnaldi, D.; Campus, C.; Ferrara, M.; Famà, F.; Picco, A.; De Carli, F.; Accardo, J.; Brugnolo, A.; Sambuceti, G.; Morbelli, S.; et al. What Predicts Cognitive Decline in De Novo Parkinson's Disease? *Neurobiol. Aging* **2012**, *33*, 1127.e11–1127.e20. [CrossRef]
132. de Schipper, L.J.; Hafkemeijer, A.; van der Grond, J. Regional Structural Hippocampal Differences between Dementia with Lewy Bodies and Parkinson's Disease. *J. Park. Dis.* **2019**, *9*, 775–783. [CrossRef]
133. Borroni, B.; Premi, E.; Formenti, A. Structural and Functional Imaging Study in Dementia with Lewy Bodies and Parkinson's Disease Dementia. *Park. Relat. Disord.* **2015**, *21*, 1049–1055. [CrossRef]
134. Gazzina, S.; Premi, E.; Turrone, R.; Acosta-Cabronero, J.; Rizzetti, M.C.; Cotelli, M.S.; Gasparotti, R.; Padovani, A.; Borroni, B. Subcortical Matter in the α-Synucleinopathies Spectrum: An MRI Pilot Study. *J. Neurol.* **2016**, *263*, 1575–1582. [CrossRef]
135. Hwang, K.S.; Langley, J.; Tripathi, R.; Hu, X.P.; Huddleston, D.E. In Vivo Detection of Substantia Nigra and Locus Coeruleus Volume Loss in Parkinson's Disease Using Neuromelanin-Sensitive MRI: Replication in Two Cohorts. *PLoS ONE* **2023**, *18*, e0282684. [CrossRef]
136. Tseriotis, V.-S.; Mavridis, T.; Eleftheriadou, K.; Konstantis, G.; Chlorogiannis, D.-D.; Pavlidis, P.; Pourzitaki, C.; Arnaoutoglou, M.; Spyridon, K. Loss of the "Swallow Tail Sign" on Susceptibility-Weighted Imaging in the Diagnosis of Dementia with Lewy Bodies: A Systematic Review and Meta-Analysis. *J. Neurol.* **2024**, *271*, 3754–3763. [CrossRef]
137. Eisenstein, T.; Groenewald, K.; van Hillegondsberg, L.; Al Hajraf, F.; Zerenner, T.; Lawton, M.A.; Ben-Shlomo, Y.; Griffanti, L.; Hu, M.T.; Klein, J.C. Cholinergic Degeneration in Prodromal and Early Parkinson's Disease: A Link to Present and Future Disease States. *Brain* **2026**, *149*, 226–237. [CrossRef]
138. Železníková, Ž.; Nováková, L.; Vojtíšek, L.; Brabenec, L.; Mitterová, K.; Morávková, I.; Rektorová, I. Early Changes in the Locus Coeruleus in Mild Cognitive Impairment with Lewy Bodies. *Mov. Disord.* **2025**, *40*, 276–284. [CrossRef]
139. Diaz-Galvan, P. Substantia Nigra Iron Deposition in Lewy Body Disease: A Magnetic Resonance Imaging and Neuropathology Study. *Mov. Disord.* **2025**, *40*, 2129–2138. [CrossRef]
140. Chen, Q. MRI Quantitative Susceptibility Mapping of the Substantia Nigra as an Early Biomarker for Lewy Body Disease. *J. Neuroimaging* **2021**, *31*, 1020–1027. [CrossRef]
141. Bhome, R. Quantitative Susceptibility Mapping Reveals Differences between Subtypes of Lewy Body Dementia. *Brain* **2026**, *149*, 1058–1069. [CrossRef]
142. Hohenfeld, C.; Werner, C.J.; Reetz, K. Resting-State Connectivity in Neurodegenerative Disorders: Is There Potential for an Imaging Biomarker? *Neuroimage Clin.* **2018**, *18*, 849–870. [CrossRef]
143. Tang, S.; Wang, Y.; Liu, Y. Large-Scale Network Dysfunction in α-Synucleinopathy: A Meta-Analysis of Resting-State Functional Connectivity. *EBioMedicine* **2022**, *77*, 103915. [CrossRef]
144. Habich, A.; Wahlund, L.O.; Westman, E.; Dierks, T.; Ferreira, D. (Dis-)Connected Dots in Dementia with Lewy Bodies—A Systematic Review of Connectivity Studies. *Mov. Disord.* **2023**, *38*, 4–15. [CrossRef]
145. Filippi, M.; Spinelli, E.G.; Cividini, C.; Agosta, F. Resting State Dynamic Functional Connectivity in Neurodegenerative Conditions: A Review of MRI Findings. *Front. Neurosci.* **2019**, *13*, 657. [CrossRef]
146. Peraza, L.R.; Colloby, S.J.; Firbank, M.J. Resting State in Parkinson's Disease Dementia and Dementia with Lewy Bodies: Commonalities and Differences. *Int. J. Geriatr. Psychiatry* **2015**, *30*, 1135–1146. [CrossRef]
147. Schumacher, J.; Thomas, A.J.; Peraza, L.R.; Firbank, M.; O'Brien, J.T.; Taylor, J.P. Functional Connectivity of the Nucleus Basalis of Meynert in Lewy Body Dementia and Alzheimer's Disease. *Int. Psychogeriatr.* **2021**, *33*, 89–94. [CrossRef]
148. Montaser-Kouhsari, L.; Young, C.B.; Poston, K.L. Neuroimaging Approaches to Cognition in Parkinson's Disease. *Prog. Brain Res.* **2022**, *269*, 257–286. [CrossRef]

149. Lowther, E.R.; O'Brien, J.T.; Firbank, M.J.; Blamire, A.M. Lewy Body Compared with Alzheimer Dementia Is Associated with Decreased Functional Connectivity in Resting State Networks. *Psychiatry Res. Neuroimaging* **2014**, *223*, 192–201. [CrossRef]
150. Chabran, E.; Roquet, D.; Gounot, D.; Sourty, M.; Armspach, J.-P.; Blanc, F. Functional Disconnectivity during Inter-Task Resting State in Dementia with Lewy Bodies. *Dement. Geriatr. Cogn. Disord.* **2018**, *45*, 105–120. [CrossRef]
151. de Macedo, B.A.; Kakadiya, J.; Maciel, R.C.; Verdan, S.; Antunes, V.; Sair, H.I.; Luna, L.P. Resting-State Functional Connectivity Alterations in Dementia with Lewy Bodies: A Systematic Review and Activation Likelihood Estimation Meta-Analysis. *Brain Imaging Behav.* **2026**, *20*, 68. [CrossRef]
152. Law, Z.K.; Todd, C.; Mehraram, R. The Role of EEG in the Diagnosis, Prognosis and Clinical Correlations of Dementia with Lewy Bodies—A Systematic Review. *Diagnostics* **2020**, *10*, 616. [CrossRef]
153. Chatzikonstantinou, S.; McKenna, J.; Karantali, E.; Petridis, F.; Kazis, D.; Mavroudis, I. Electroencephalogram in Dementia with Lewy Bodies: A Systematic Review. *Aging Clin. Exp. Res.* **2021**, *33*, 1197–1208. [CrossRef]
154. Bonanni, L.; Thomas, A.; Tiraboschi, P.; Perfetti, B.; Varanese, S.; Onofrj, M. EEG Comparisons in Early Alzheimer's Disease, Dementia with Lewy Bodies and Parkinson's Disease with Dementia Patients with a 2-Year Follow-Up. *Brain* **2008**, *131*, 690–705. [CrossRef]
155. Franciotti, R.; Pilotto, A.; Moretti, D.V.; Falasca, N.W.; Arnaldi, D.; Taylor, J.P.; Nobili, F.; Kramberger, M.; Ptacek, S.G.; Padovani, A.; et al. Anterior EEG Slowing in Dementia with Lewy Bodies: A Multicenter European Cohort Study. *Neurobiol. Aging* **2020**, *93*, 55–60. [CrossRef]
156. Stylianou, M.; Murphy, N.; Peraza, L.R. Quantitative Electroencephalography as a Marker of Cognitive Fluctuations in Dementia with Lewy Bodies and an Aid to Differential Diagnosis. *Clin. Neurophysiol.* **2018**, *129*, 1209–1220. [CrossRef]
157. Zinno, L.; Negrotti, A.; Falzoi, C.; Messa, G.; Goldoni, M.; Calzetti, S. Generalized Rhythmic Delta Activity Frontally Predominant Differentiates Dementia with Lewy Bodies from Alzheimer's Disease and Parkinson's Disease Dementia. *Clin. EEG Neurosci.* **2022**, *53*, 426–434. [CrossRef]
158. Schumacher, J.; Taylor, J.P.; Hamilton, C.A. Quantitative EEG as a Biomarker in Mild Cognitive Impairment with Lewy Bodies. *Alzheimer's Res. Ther.* **2020**, *12*, 82. [CrossRef]
159. Matar, E.; Shine, J.M.; Halliday, G.M.; Lewis, S.J.G. Cognitive Fluctuations in Lewy Body Dementia: Towards a Pathophysiological Framework. *Brain* **2020**, *143*, 31–46. [CrossRef]
160. Minoshima, S.; Cross, D.; Thientunyakit, T.; Foster, N.L.; Drzezga, A. 18F-FDG PET Imaging in Neurodegenerative Dementing Disorders: Insights into Subtype Classification, Emerging Disease Categories, and Mixed Dementia with Copathologies. *J. Nucl. Med.* **2022**, *63*, 2S–12S. [CrossRef]
161. Rennie, A. Cerebrovascular and Alzheimer's Disease Biomarkers in Dementia with Lewy Bodies and Other Dementias. *Brain Commun.* **2024**, *6*, fcae290. [CrossRef]
162. Cohen, J.S.; Phillips, J.; Das, S.R.; Olm, C.A.; Radhakrishnan, H.; Rhodes, E.; Cousins, K.A.Q.; Xie, S.X.; Nasrallah, I.M.; Yushkevich, P.A.; et al. Posterior Hippocampal Sparing in Lewy Body Disorders with Alzheimer's Copathology: An In Vivo MRI Study. *Neuroimage Clin.* **2024**, *45*, 103714. [CrossRef]
163. Donaghy, P.C.; Firbank, M.J.; Thomas, A.J.; Lloyd, J.; Petrides, G.; Barnett, N.; Olsen, K.; O'Brien, J.T. Clinical and Imaging Correlates of Amyloid Deposition in Dementia with Lewy Bodies. *Mov. Disord.* **2018**, *33*, 1130–1138. [CrossRef]
164. Singh, N.A.; Goodrich, A.W.; Graff-Radford, J.; Machulda, M.M.; Sintini, I.; Carlos, A.F.; Robinson, C.G.; Reid, R.I.; Lowe, V.J.; Jack, C.R.; et al. Altered Structural and Functional Connectivity in Posterior Cortical Atrophy and Dementia with Lewy Bodies. *Neuroimage* **2024**, *290*, 120564. [CrossRef]
165. Conti, M.; Mascioli, D.; Simonetta, C.; Ferrari, V.; Bissacco, J.; Bagetta, S.; Carparelli, F.; Bernardini, S.; Di Giuliano, F.; Marchionni, E.; et al. Clinical, Biological, and Functional Connectivity Profile of Patients with De Novo Parkinson Disease Who Are *APOE* E4 Carriers. *Neurology* **2026**, *106*, e214449. [CrossRef]
166. Fathy, Y.Y.; Jonkman, L.E.; Bol, J.J.; Timmermans, E.; Jonker, A.J.; Rozemuller, A.J.M.; van de Berg, W.D.J. Axonal Degeneration in the Anterior Insular Cortex Is Associated with Alzheimer's Co-Pathology in Parkinson's Disease and Dementia with Lewy Bodies. *Transl. Neurodegener.* **2022**, *11*, 52. [CrossRef]
167. Jellinger, K.A. Pathobiology of Cognitive Impairment in Parkinson Disease: Challenges and Outlooks. *Int. J. Mol. Sci.* **2023**, *25*, 498. [CrossRef]
168. Ferreira, D.; Przybelski, S.A.; Lesnick, T.G.; Diaz-Galvan, P.; Schwarz, C.G.; Murray, M.M.; Dickson, D.W.; Nguyen, A.; Reichard, R.R.; Senjem, M.L.; et al. Longitudinal FDG-PET Metabolic Change Along the Lewy Body Continuum. *JAMA Neurol.* **2025**, *82*, 285–294. [CrossRef]
169. Mak, E. Influence of Alpha-Synuclein on Glucose Metabolism in Alzheimer's Disease Continuum: Analyses of Alpha-Synuclein Seed Amplification Assay and FDG-PET. *Alzheimer's Dement.* **2025**, *21*, e14571. [CrossRef]
170. Nakamura, K.; Tagai, K.; Shinotoh, H.; Hirano, S.; Shimada, H. Concurrent Alzheimer's Disease Pathologies in Lewy Body Diseases Affect Cognition and Glucose Metabolism in the Posterior Cingulate Gyrus: A Multimodal PET Study. *J. Alzheimer's Dis.* **2025**, *106*, 1074–1086. [CrossRef]

171. Edison, P.; Ahmed, I.; Fan, Z.; Hinz, R.; Gelosa, G.; Ray Chaudhuri, K.; Walker, Z.; Turkheimer, F.E.; Brooks, D.J. Microglia, Amyloid, and Glucose Metabolism in Parkinson's Disease with and without Dementia. *Neuropsychopharmacology* **2013**, *38*, 938–949. [CrossRef]
172. Lavrova, A.; Pham, N.T.T.; Vernon, C.J.; Carlos, A.F.; Petersen, R.C.; Dickson, D.W.; Lowe, V.J.; Jack, C.R.; Whitwell, J.L.; Josephs, K.A. A Multimodal Clinical Diagnostic Approach Using MRI and 18F-FDG-PET for Antemortem Diagnosis of TDP-43 in Cases with Low-Intermediate Alzheimer's Disease Neuropathologic Changes and Primary Age-Related Tauopathy. *J. Neurol.* **2024**, *271*, 4105–4118. [CrossRef]
173. Duong, M.T.; Wolk, D.A. Limbic-Predominant Age-Related TDP-43 Encephalopathy: LATE-Breaking Updates in Clinicopathologic Features and Biomarkers. *Curr. Neurol. Neurosci. Rep.* **2022**, *22*, 689–698. [CrossRef]
174. Bauer, C.E.; Zachariou, V.; Sudduth, T.L.; Van Eldik, L.J.; Jicha, G.A.; Nelson, P.T.; Wilcock, D.M.; Gold, B.T. Plasma TDP-43 Levels Are Associated with Neuroimaging Measures of Brain Structure in Limbic Regions. *Alzheimer's Dement.* **2023**, *15*, e12437. [CrossRef]
175. Khalil, M.; Teunissen, C.E.; Lehmann, S.; Otto, M.; Piehl, F.; Ziemssen, T.; Bittner, S.; Sormani, M.P.; Gattringer, T.; Abu-Rumeileh, S.; et al. Neurofilaments as Biomarkers in Neurological Disorders—Towards Clinical Application. *Nat. Rev. Neurol.* **2024**, *20*, 269–287. [CrossRef]
176. Batzu, L.; Rota, S.; Hye, A.; Heslegrave, A.; Trivedi, D.; Gibson, L.L.; Farrell, C.; Podlewska, A.M.; Chaudhuri, K.R.; Aarsland, D. Plasma P-Tau181, Neurofilament Light Chain and Association with Cognition in Parkinson's Disease. *npj Park. Dis.* **2022**, *8*, 154. [CrossRef]
177. Gibson, L.L.; Pollak, T.A.; Heslegrave, A.; Hye, A.; Batzu, L.; Rota, S.; Trivedi, D.; Nicholson, T.R.; Ffytche, D.; Zetterberg, H.; et al. Plasma Neurofilament Light and P-Tau181 and Risk of Psychosis in Parkinson's Disease. *J. Park. Dis.* **2022**, *12*, 1527–1538. [CrossRef]
178. Yan, S.; Sahoo, A.; Zerenner, T.; Marek, K.; Sommerauer, M.; Oertel, W.; Hu, M.T.; Tofaris, G.K. Serum P-Tau217 Is a Prognostic Indicator of Cognitive Impairment in Idiopathic REM Sleep Behavior Disorder. *Ann. Neurol.* **2026**, *99*, 912–921. [CrossRef]
179. Rousset, R.Z.; Honey, M.I.J.; den Braber, A.; van der Flier, W.M.; Holstege, H.; Lorenz, L.; Wessels, M.H.J.; Killestein, J.; Huisman, M.; Kok, A.; et al. Glial Fibrillary Acidic Protein and Neurofilament Light Reference Intervals in Healthy Individuals. *JAMA Netw. Open* **2026**, *9*, e2612793. [CrossRef]
180. Carson, R.E.; Naganawa, M.; Toyonaga, T.; Koohsari, S.; Yang, Y.; Chen, M.-K.; Matuskey, D.; Finnema, S.J. Imaging of Synaptic Density in Neurodegenerative Disorders. *J. Nucl. Med.* **2022**, *63*, 60S–67S. [CrossRef]
181. Andersen, K.B.; Hansen, A.K.; Damholdt, M.F.; Horsager, J.; Skjaerbaek, C.; Gottrup, H.; Klit, H.; Schacht, A.C.; Danielsen, E.H.; Brooks, D.J.; et al. Reduced Synaptic Density in Patients with Lewy Body Dementia: An [11C]UCB-J PET Imaging Study. *Mov. Disord.* **2021**, *36*, 2057–2065. [CrossRef]
182. Martin, S.L.; Uribe, C.; Desmond, K.L.; Narciso, L.; Dolman, B.; Torres-Carmona, E.; Boileau, I.; Graff-Guerrero, A.; Vasdev, N.; Strafella, A.P. [18F]SynVest-1 PET Imaging in People with Parkinson's Disease. *Brain Commun.* **2025**, *7*, fcaf258. [CrossRef]
183. Vanderlinden, G.; Carron, C.; Van Opstal, J.; Cohilis, M.; Vandenberghe, W.; Koole, M.; Van Laere, K. Quantification of 18F-SynVesT-1 Binding in Healthy Aging and Head-to-Head Comparison with 11C-UCB-J. *J. Cereb. Blood Flow Metab.* **2026**, *46*, 2426–2435. [CrossRef]
184. Andersen, K.B.; Hansen, A.K.; Schacht, A.C.; Horsager, J.; Gottrup, H.; Klit, H.; Danielsen, E.H.; Poston, K.L.; Pavese, N.; Brooks, D.J.; et al. Synaptic Density and Glucose Consumption in Patients with Lewy Body Diseases: An [11C]UCB-J and [18F]FDG PET Study. *Mov. Disord.* **2023**, *38*, 796–805. [CrossRef]
185. Kreisl, W.C.; Henter, I.D.; Innis, R.B. Imaging Translocator Protein as a Biomarker of Neuroinflammation in Dementia. *Adv. Pharmacol.* **2018**, *82*, 163–185. [CrossRef]
186. Surendranathan, A.; Su, L.; Mak, E.; Passamonti, L.; Hong, Y.T.; Arnold, R.; Vázquez Rodríguez, P.; Bevan-Jones, W.R.; Brain, S.A.E.; Fryer, T.D.; et al. Early Microglial Activation and Peripheral Inflammation in Dementia with Lewy Bodies. *Brain* **2018**, *141*, 3415–3427. [CrossRef]
187. Kouli, A.; Spindler, L.R.B.; Fryer, T.D.; Hong, Y.T.; Malpetti, M.; Aigbirhio, F.I.; White, S.R.; Camacho, M.; O'Brien, J.T.; Williams-Gray, C.H. Neuroinflammation Is Linked to Dementia Risk in Parkinson's Disease. *Brain* **2024**, *147*, 923–935. [CrossRef]
188. Scott, K.M.; Spindler, L.R.B.; Peattie, A.R.D.; Kouli, A.; Fryer, T.D.; Hong, Y.T.; Camacho, M.; Solim, I.; Kahanawita, L.; Williams-Gray, C.H. Multimodal Markers of Immune Activation Predict Cognitive Outcomes in Parkinson's Disease. *Brain Behav. Immun.* **2025**, *129*, 165–178. [CrossRef]
189. Young, P.N.E.; Estarellas, M.; Coomans, E.; Srikrishna, M.; Beaumont, H.; Maass, A.; Venkataraman, A.V.; Lissaman, R.; Jiménez, D.; Betts, M.J.; et al. Imaging Biomarkers in Neurodegeneration: Current and Future Practices. *Alzheimer's Res. Ther.* **2020**, *12*, 49. [CrossRef]
190. Quadalti, C.; Calandra-Buonaura, G.; Baiardi, S.; Mastrangelo, A.; Rossi, M.; Zenesini, C.; Giannini, G.; Candelise, N.; Sambati, L.; Polischi, B.; et al. Neurofilament Light Chain and α-Synuclein RT-QuIC as Differential Diagnostic Biomarkers in Parkinsonisms and Related Syndromes. *npj Park. Dis.* **2021**, *7*, 93. [CrossRef]

191. Miyagawa, T.; Przybelski, S.A.; Maltais, D. The Value of Multimodal Imaging with 123I-FP-CIT SPECT in Differential Diagnosis of Dementia with Lewy Bodies and Alzheimer's Disease Dementia. *Neurobiol. Aging* **2021**, *99*, 11–18. [CrossRef]
192. Bhome, R.; Verdi, S.; Martin, S.A.; Hannaway, N.; Dobreva, I.; Oxtoby, N.P.; Leal, G.C.; Rutherford, S.; Marquand, A.F.; Weil, R.S.; et al. A neuroimaging measure to capture heterogeneous patterns of atrophy in Parkinson's disease and dementia with Lewy bodies. *Neuroimage Clin.* **2024**, *42*, 103596. [CrossRef]
193. Joza, S.; Delva, A.; Tremblay, C. Distinct Brain Atrophy Progression Subtypes Underlie Phenoconversion in Isolated REM Sleep Behaviour Disorder. *EBioMedicine* **2025**, *117*, 105753. [CrossRef]
194. Perovnik, M.; Simončič, U.; Jamšek, J.; Kramberger, M.G.; Brumberg, J.; Meyer, P.; Perani, D.; Caminiti, S.; Brendel, M.; Stockbauer, A.; et al. Metabolic Brain Networks in Dementia with Lewy Bodies: From Prodromal to Manifest Disease Stages. *J. Neurol. Neurosurg. Psychiatry* **2025**, *97*, 316–324. [CrossRef]
195. Goldman, J.G.; Boeve, B.F.; Galasko, D. Implications and Opportunities Regarding Biological Frameworks in Overt and Prodromal Dementia with Lewy Bodies. *Alzheimer's Dement.* **2025**, *21*, e70470. [CrossRef]
196. Sarro, L.; Senjem, M.L.; Lundt, E.S.; Przybelski, S.A.; Lesnick, T.G.; Graff-Radford, J.; Boeve, B.F.; Lowe, V.J.; Ferman, T.J.; Knopman, D.S.; et al. Amyloid-β Deposition and Regional Grey Matter Atrophy Rates in Dementia with Lewy Bodies. *Brain* **2016**, *139*, 2740–2750. [CrossRef]
197. Blanc, F.; Bouteloup, V.; Paquet, C.; Chupin, M.; Pasquier, F.; Gabelle, A.; Ceccaldi, M.; de Sousa, P.L.; Krolak-Salmon, P.; David, R.; et al. Cognitive and Neuroimaging Outcome of Very Prodromal Dementia with Lewy Bodies. *Geroscience* **2025**, *48*, 1051–1062. [CrossRef]
198. Musso, G.; Fiorenzato, E.; Misenti, V.; Cauzzo, S.; Biundo, R.; Fogliano, C.; Bonato, G.; Meissner, W.; Campagnolo, M.; Carecchio, M.; et al. Detecting Amyloid and Tau Pathology in Parkinson's Disease, 4R-Tauopathies and Control Subjects with Plasma PTau217. *Front. Neurol.* **2025**, *16*, 1638852. [CrossRef]
199. Gibson, L.; Abdelnour, C.; Chong, J.; Ballard, C.; Aarsland, D. Clinical Trials in Dementia with Lewy Bodies: The Evolving Concept of Co-Pathologies, Patient Selection and Biomarkers. *Curr. Opin. Neurol.* **2023**, *36*, 264–275. [CrossRef]
200. Brown, C.A.; Mundada, N.S.; Cousins, K.A.Q.; Sadeghpour, N.; Lyu, X.; McGrew, E.; Korecka, M.; Chen-Plotkin, A.; Xie, L.; Wisse, L.E.M.; et al. Evaluation of Copathology and Clinical Trajectories in Individuals with Tau-Clinical Mismatch. *JAMA Neurol.* **2026**, *83*, 126–136. [CrossRef]
201. Cummings, J.; Apostolova, L.; Rabinovici, G.D. Lecanemab: Appropriate Use Recommendations. *J. Prev. Alzheimer's Dis.* **2023**, *10*, 362–377. [CrossRef]
202. Rabinovici, G.D.; Selkoe, D.J.; Schindler, S.E.; Aisen, P.; Apostolova, L.G.; Atri, A.; Greenberg, S.M.; Hendrix, S.B.; Petersen, R.C.; Weiner, M.; et al. Donanemab: Appropriate Use Recommendations. *J. Prev. Alzheimer's Dis.* **2025**, *12*, 100150. [CrossRef]
203. Kluge, A.; Schaeffer, E.; Bunk, J.; Sommerauer, M.; Röttgen, S.; Schulte, C.; Roeben, B.; von Thaler, A.-K.; Welzel, J.; Lucius, R.; et al. Detecting Misfolded α-Synuclein in Blood Years before the Diagnosis of Parkinson's Disease. *Mov. Disord.* **2024**, *39*, 1289–1299. [CrossRef]
204. Martinez-Valbuena, I.; Emamikhah, M.; Olszewska, D.A.; Weber, S.K.; Schnell, S.; Fereshtehnejad, S.-M.; Reyes, N.G.D.; Sousa, M.; Di Luca, D.G.; Ta, J.; et al. A Multimodal Biomarker Strategy to Enhance Diagnostic Precision in Neurodegenerative Parkinsonism. *Nat. Med.* **2026**, *32*, 2073–2082. [CrossRef]
205. Bräuer, S.; Sondermann, V.; Schniewind, I.; Hähnel, T.; Dinter, E.; Kleineidam, L.; Stark, M.; Schmid, M.; Sodenkamp, S.; Laske, C.; et al. Alpha-Synuclein Quantitative Seed Amplification Assay Predicts Conversion to Dementia. *Alzheimer's Dement.* **2026**, *22*, e71167. [CrossRef]
206. Wang, D.; Honnorat, N.; Toledo, J.B.; Li, K.; Charisis, S.; Rashid, T.; Benet Nirmala, A.; Brandigampala, S.R.; Mojtabai, M.; Seshadri, S.; et al. Deep Learning Reveals Pathology-Confirmed Neuroimaging Signatures in Alzheimer's, Vascular and Lewy Body Dementias. *Brain* **2025**, *148*, 1963–1977. [CrossRef]
207. Xu, Y.; Denkinger, M.N.; Liu, M.; Gong, K.; Chen, Y.; Western, D.; Timsina, J.; Cheng, Y.; Xie, Y.; Mu, R.; et al. GPND-AI NULISA: A 15-Protein AI Classifier for Diagnosis and Co-Pathology Profiling across Neurodegenerative Diseases. *Alzheimer's Dement.* **2026**, *22*, e71420. [CrossRef]
208. Ono, D.; Sekiya, H.; Maier, A.R.; Graff-Radford, N.R.; Wszolek, Z.K.; Dickson, D.W. Chronological Diagnostic Algorithm Predicting Neuropathology in Parkinsonism. *Ann. Neurol.* **2026**, *99*, 1405–1414. [CrossRef]
209. Xia, C.A.; Salarian, M.; Gartshore, C.J.; Scaglione, A.; Hayes, T.; Liu, S.; Tsai, H.-M.; Echavarren, J.; Cid, J.M.; Matzeu, A.; et al. Development and Characterization of a Novel TDP-43 Positron Emission Tomography Tracer: [18F]JNJ-TDP43-1. *Alzheimer's Dement.* **2026**, *22*, e71675. [CrossRef]

Disclaimer/Publisher's Note: The statements, opinions and data contained in all publications are solely those of the individual author(s) and contributor(s) and not of MDPI and/or the editor(s). MDPI and/or the editor(s) disclaim responsibility for any injury to people or property resulting from any ideas, methods, instructions or products referred to in the content.